AD NUMBER

AD875847

NEW LIMITATION CHANGE

TO

Approved for public release, distribution unlimited

FROM

Distribution authorized to U.S. Gov't. agencies and their contractors; Critical Technology; SEP 1970. Other requests shall be referred to Army Electronics Command, Fort Monmouth, NJ.

AUTHORITY

USAEC ltr, 23 Sep 1971

RESEARCH AND DEVELOPMENT TECHNICAL REPORT
ECOM-0381-4

EVALUATION OF ATMOSPHERIC TRANSPORT AND DIFFUSION

SEMI-ANNUAL REPORT

By

Tom E. Sanford, Principal Investigator

September 1970

ECOM

UNITED STATES ARMY ELECTRONICS COMMAND · FORT MONMOUTH, N.J.
Contract DAAB07-68-C-0381
DEPARTMENTS OF METEOROLOGY AND OCEANOGRAPHY
TEXAS A&M UNIVERSITY
College Station, Texas 77843

Reports Control Symbol
OSD - 1366

Technical Report ECOM-0381-4

September 1970

EVALUATION OF

ATMOSPHERIC TRANSPORT AND DIFFUSION

Semi-Annual Report

15 December 1969 to 15 June 1970

Report No. 4

Contract No. DAAB07-68-C-0381

Project 586

Reference 70-9-T

Tom E. Sanford, Principal Investigator

TEXAS A & M RESEARCH FOUNDATION

College Station, Texas

For

U. S. Army Electronics Command, Fort Monmouth, New Jersey

Distribution Statement

This document is subject to special controls and each transmittal to foreign governments or foreign nationals may be made only with prior approval of CG, U. S. Army Electronics Command, Fort Monmouth, New Jersey, ATTN: AMSEL-BL-FM-T

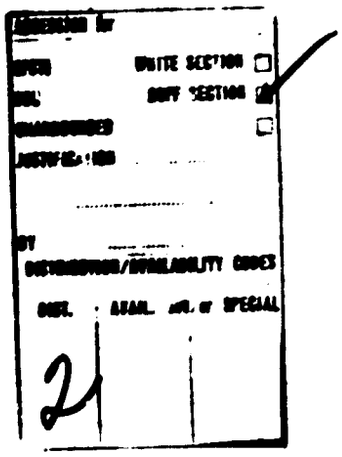

NOTICES

Disclaimers

The findings in this report are not to be construed as an official Department of the Army position, unless so designated by other authorized documents. The citation of trade names and names of manufacturers in this report is not to be construed as official Government indorsement or approval of commercial products or services referenced herein.

Disposition

Destroy this report when it is no longer needed. Do not return it to the originator.

ABSTRACT

This report contains a summary of the activities carried out under Signal Corps Contract No. DAAB07-68-C-0381 (Texas A & M Research Foundation Project No. 586) during the contract period 15 December 1969 to 15 June 1970.

Activities during this period have been devoted primarily to the programming of the equations for the forested boundary layer and the wiring and checking of the computer patchboards for solution of these equations on the general purpose analog computer at Texas A&M University. The complete set of these equations scaled in analog format is included in this report as are wiring diagrams for solution of the scaled equations.

ACKNOWLEDGEMENT

The research reported herein has been performed under Contract DAAB07-68-C-0381, sponsored by the U. S. Army Electronics Laboratories at Fort Monmouth, New Jersey; however, personnel and equipment support for the General Purpose Analog Computer facility utilized in this research are also provided by the Research Council of Texas A&M University.

TABLE OF CONTENTS

LIST OF TABLES

I. Introduction

An experimental set of equations for simulating the atmosphere within and above a tropical forest is under development at Texas A&M University. The general analog format of these equations is presented in Appendix B of Technical Report ECOM-0381-3, April 1970, under Contract DAAB07-68-C-0381. The complete set of tentatively scaled equations for the tropical forest system was set forth in that report. The time scaling used in the initial simulation was a computer-time versus real-time factor of 1440 to 1; that is, the computer solution is 1440 times faster than real time, so that a 12-hr solution is obtained in 30 sec.

The principal activities during this reporting period have been devoted to the task of modifying some of the scaling factors initially employed in programming the equations for solution on the General Purpose Analog Computer at Texas A&M and to wiring of the computer patchboards.

Section II of this report contains the modified scale factors and constants employed in the forest and boundary layer simulation. Section III contains a complete set of equations scaled for the new scale factors, and Section IV contains the analog computer program for solution of the equations.

II. Scale Factors and Constants Employed in the Forest Boundary Layer Simulation

A complete list of scale factors and constants employed in the forest boundary simulation is shown in Table 1. A significant modification has been made to the scale factors for the east-west and north-south components of the wind in the free air above the forest. These wind components were initially scaled for 50 m/sec in the free air and 10 m/sec within the forest. This value of 50 m/sec is certainly far in excess of what would normally be expected in tropical areas, except in very extreme circumstances, such as in a hurricane or typhoon; therefore, the east-west and north-south components of the wind and free air have been rescaled to 25 m/sec. The value of 10 m/sec within the forest has been retained. For dense tropical forests, this value is considered to be extremely high; however, for relatively open forests, the value is not considered to be excessively large, especially near the edges of such forests.

The east-west and north-south components of the shearing stress have been rescaled similarly from 20 dynes/cm^2 to 10 dynes/cm^2. This value is more consistent with the rescaled value for the east-west and north-south components of the wind. The other scale factors remain unchanged, as do the fixed constants shown in Section B of Table 1. These scale factors also can be considered as tentative since modification may be anticipated subsequent to obtaining an initial solution of the equations on the general purpose analog computer.

Table 1. Scale factors and constants employed in the forest boundary layer simulation.

A. Scale Factors

D_A	: 10 cm/sec	R_N	: .05 cal/cm^{2}sec
e	: 100 mb	S_A	: 2000 cm/sec
F_x,F_y	: 10 dynes/cm^3	$S_{A'}$	: 1000 cm/sec
FCC	: 100 cm/km	T	: 50°C
ICC	: 100 cm/km	time	: 1440:1
K_m	: 50,000 cm^2/sec	u,v	: 2500 cm/sec (free air)
q_c	: .05 cal/cm^{2}sec		: 1000 cm/sec (forest)
q_e	: .05 cal/cm^{2}sec	τ_x,τ_y	: 10 dynes/cm^2

B. Constants

a = .621	P = 86,400 sec
C_p = .24 cal/gm deg	p_o = 1012 mb
g = 980 cm/sec^2	Z = 1050 m
I = .0330 cal/cm^{2}sec	σ = 1.354x10^{-12} cal/cm^{2}sec deg^4
k = .40	ω = 7.3x10^{-5} rad/sec
L = 593.3 cal/gm	ρ = 1.2x10^{-3} gm/cm^3

III. Scaled Analog Format of the Equations Employed in the Forest Simulation

Table 2 contains the complete expanded set of the newly scaled equations. Columns 1 and 2 in Table 2, headed j and i, are indices which refer to the particular layer of applicability of the equation involved. The third column, headed z_i, indicates the nominal height in meters of the layer to which the individual equation applies. Similarly, column 4, headed z_{ij}, contains the applicable height in meters of the layer interfaces at which the fluxes of momentum, heat, and vapor pressure are calculated, and column 5 contains the scaled equations themselves. The numbers in parentheses appearing on the extreme right of the equations are reference numbers, corresponding to the equation numbers given in Semi-Annual Report No. 3 on Project 586, Contract No. DAAB07-68-0381.

The complete set of equations is shown here to facilitate understanding of the computer solution diagrams shown in Section IV. The coefficients, c, for these equations are tabulated in Table 3 for easy reference. Some of the values of c appearing in this table differ from those given in the aforementioned report. These differences have resulted from the selection of new scale factors for the east-west and north-south components of the wind and for the shearing stresses. The scaled equations have been written so that the scale factors are shown explicitly for each variable. For example, in equation (s1), at the level of 250 m, the east-west component of the wind is scaled for a maximum value of 2500 cm/sec and the time scale factor is 1440:1; thus, the equation is divided by 2500 and multiplied by the

Table 2. Scaled equations for forest boundary layer simulation. Coefficients, c, are given in Table 3.

j	i	z_j (m)	z_{ij} (m)	A. Free air, $z \geq (d + \Lambda)$
7		250m		$1440\left(\frac{u_7}{2500}\right) = \int \left[-\frac{.4g\left(\frac{\partial h}{\partial x}\right)_o}{.6944} - \frac{\Delta\left(g\frac{\partial h}{\partial x}\right)_7}{1.736} + c_1\left(\frac{v_7}{2500}\right) + c'_{2,7}\left(\frac{\tau_{x,67}}{10}\right) - \left(\frac{\alpha'_7 u_7 - \beta'_7 v_7}{1.736}\right) \right] dt$
6		150		$1440\left(\frac{u_6}{2500}\right) = \int \left[-\frac{.4g\left(\frac{\partial h}{\partial x}\right)_o}{.6944} - \frac{\left(\Delta g\frac{\partial h}{\partial x}\right)_6}{1.736} + c_1\left(\frac{v_6}{2500}\right) + c_{2,6}\left(\frac{\tau_{x,67} - \tau_{x,56}}{10}\right) - c_{3,6}\left(\frac{\alpha'_4 u_4 - \beta'_4 v_4}{1.736}\right) - c_{4,6}\left(\frac{\alpha'_7 u_7 - \beta'_7 v_7}{1.736}\right) \right] dt$ (s1)
5		75		$1440\left(\frac{u_5}{2500}\right) = \int \left[-\frac{.4g\left(\frac{\partial h}{\partial x}\right)_o}{.6944} - \frac{\left(\Delta g\frac{\partial h}{\partial x}\right)_5}{1.736} + c_1\left(\frac{v_5}{2500}\right) + c_{2,5}\left(\frac{\tau_{x,56} - \tau_{x,45}}{10}\right) - c_{3,5}\left(\frac{\alpha'_4 u_4 - \beta'_4 v_4}{1.736}\right) - c_{4,5}\left(\frac{\alpha'_7 u_7 - \beta'_7 v_7}{1.736}\right) \right] dt$

Table 2. Continued

j	i	z_j (m)	z_{ij} (m)	
4		45		$1440\left(\frac{u_4}{2500}\right) = \int\left[\left[-\frac{.4g\left(\frac{\partial h}{\partial x}\right)_o}{.6944} + c_1\left(\frac{v_4}{2500}\right) + c_{2,4}\left(\frac{\tau_{x,45} - \tau_{x,d}}{10}\right) - \left(\frac{\alpha'_4 u_4 - \beta'_4 v_4}{1.736}\right)\right]\right] dt$
7		250		$1440\left(\frac{v_7}{2500}\right) = \int\left[\left[-\frac{.4g\left(\frac{\partial h}{\partial y}\right)_o}{.6944} - \frac{\left(\Delta g\frac{\partial h}{\partial y}\right)_7}{1.736} - c_1\left(\frac{u_7}{2500}\right) + c'_{2,7}\left(\frac{\tau_{y,67}}{10}\right) - \left(\frac{\alpha'_7 v_7 + \beta'_7 u_7}{1.736}\right)\right]\right] dt$
6		150		$1440\left(\frac{v_6}{2500}\right) = \int\left[\left[-\frac{.4g\left(\frac{\partial h}{\partial y}\right)_o}{.6944} - \frac{\left(\Delta g\frac{\partial h}{\partial y}\right)_6}{1.736} - c_1\left(\frac{u_6}{2500}\right) + c_{2,6}\left(\frac{\tau_{y,67} - \tau_{y,56}}{10}\right) - c_{3,6}\left(\frac{\alpha'_4 v_4 + \beta'_4 u_4}{1.736}\right) - c_{4,6}\left(\frac{\alpha'_7 v_7 + \beta'_7 u_7}{1.736}\right)\right]\right] dt$ (s2)
5		75		$1440\left(\frac{v_5}{2500}\right) = \int\left[\left[-\frac{.4g\left(\frac{\partial h}{\partial y}\right)_o}{.6944} - \frac{\left(\Delta g\frac{\partial h}{\partial y}\right)_5}{1.736} - c_1\left(\frac{u_5}{2500}\right) + c_{2,5}\left(\frac{\tau_{y,56} - \tau_{y,45}}{10}\right) - c_{3,5}\left(\frac{\alpha'_4 v_4 + \beta'_4 u_4}{1.736}\right) - c_{4,7}\left(\frac{\alpha'_7 v_7 + \beta'_7 u_7}{1.736}\right)\right]\right] dt$

Table 2. Continued

j	i	z_j (m)	z_{ij} (m)	
4		45		$1440\left(\frac{v_4}{2500}\right) = \int\left[-\frac{.4\rho\left(\frac{\partial h}{\partial y}\right)_o}{.6944} - c_1\left(\frac{u_4}{2500}\right) + c_{2,4}\left(\frac{\tau_{y,45} - \tau_{v,d}}{10}\right) - \left(\frac{\alpha_4' v_4 + \beta_4' u_4}{1.736}\right)\right] dt$ (s2)
7		250		$1440\left(\frac{T_7}{50}\right) = \int\left[\frac{R}{.03472} - c_{5,7}'\left(\frac{q_{c,67}}{.05}\right) - \left(\frac{u_7\left(\frac{\partial T}{\partial x}\right)_7 + v_7\left(\frac{\partial T}{\partial y}\right)_7}{.03472}\right)\right] dt$
6		150		$1440\left(\frac{T_6}{50}\right) = \int\left[\frac{R}{.03472} - c_{5,6}\left(\frac{q_{c,67} - q_{c,56}}{.05}\right) - c_{3,6}\left(\frac{u_4\left(\frac{\partial T}{\partial x}\right)_4 + v_4\left(\frac{\partial T}{\partial y}\right)_4}{.03472}\right)\right.$ (s3)
				$\left. - c_{4,6}\left(\frac{u_7\left(\frac{\partial T}{\partial x}\right)_7 + v_7\left(\frac{\partial T}{\partial y}\right)_7}{.03472}\right)\right] dt$

Table 2. Continued

j	i	z_j (m)	z_{ij} (m)	
5		75		$1440\left(\frac{T_5}{50}\right) = \int \left[\frac{R}{.03472} - c_{5,5}\left(\frac{q_{c,56} - q_{c,45}}{.05}\right) - c_{3,5}\left(\frac{u_4\left(\frac{\partial T}{\partial x}\right)_4 + v_4\left(\frac{\partial T}{\partial y}\right)_4}{.03472}\right) - c_{4,5}\left(\frac{u_7\left(\frac{\partial T}{\partial x}\right)_7 + v_7\left(\frac{\partial T}{\partial y}\right)_7}{.03472}\right)\right] dt$ (s3)
4		50		$1440\left(\frac{T_4}{50}\right) = \int \left[\frac{R}{.03472} - c_{5,4}\left(\frac{q_{c,45} - q_{c,d+}}{.05}\right) - \left(\frac{u_4\left(\frac{\partial T}{\partial x}\right)_4 + v_4\left(\frac{\partial T}{\partial y}\right)_4}{.03472}\right)\right] dt$	
7		250		$1440\left(\frac{e_7}{100}\right) = \int \left[-c'_{6,7}\left(\frac{q_{e,67}}{.05}\right) - \left(\frac{u_7\left(\frac{\partial e}{\partial x}\right)_7 + v_7\left(\frac{\partial e}{\partial y}\right)_7}{.06944}\right)\right] dt$	
6		150		$1440\left(\frac{e_6}{100}\right) = \int \left[-c_{6,6}\left(\frac{q_{e,67} - q_{e,56}}{.05}\right) - c_{3,6}\left(\frac{u_4\left(\frac{\partial e}{\partial x}\right)_4 + v_4\left(\frac{\partial e}{\partial y}\right)_4}{.06944}\right) - c_{4,6}\left(\frac{u_7\left(\frac{\partial e}{\partial x}\right)_7 + v_7\left(\frac{\partial e}{\partial y}\right)_7}{.06944}\right)\right] dt$ (s4)

Table 2. Continued

j	i	z_j (m)	z_{ij} (m)	
5		75		$1440\left(\frac{e_5}{100}\right) = \int \left[- c_{6,5}\left(\frac{\eta_{e,56} - \eta_{e,45}}{.05}\right) - c_{3,5}\left(\frac{u_4\left(\frac{\partial e}{\partial x}\right)_4 + v_4\left(\frac{\partial e}{\partial y}\right)_4}{.06944}\right) - c_{4,5}\left(\frac{u_7\left(\frac{\partial e}{\partial x}\right)_7 + v_7\left(\frac{\partial e}{\partial y}\right)_7}{.06944}\right)\right] dt$ (s4)
4		45		$1440\left(\frac{e_4}{100}\right) = \int \left[- c_{6,4}\left(\frac{\eta_{e,45} - \eta_{e,d+}}{.05}\right) - \left(\frac{u_4\left(\frac{\partial e}{\partial x}\right)_4 + v_4\left(\frac{\partial e}{\partial y}\right)_4}{.06944}\right)\right] dt$
7	6		200	$\left(\frac{\tau_{x,67}}{10}\right) = c_{7,7}\left(\frac{K_{m,4}}{50,000}\right)\left(\frac{u_7 - u_6}{2500}\right)$
6	5		100	$\left(\frac{\tau_{x,56}}{10}\right) = c_{7,6}\left(\frac{K_{m,4}}{50,000}\right)\left(\frac{u_6 - u_5}{2500}\right)$ (s7)
5	4		50	$\left(\frac{\tau_{x,45}}{10}\right) = c_{7,5}\left(\frac{K_{m,4}}{50,000}\right)\left(\frac{u_5 - u_4}{2500}\right)$
7	6		200	$\left(\frac{\tau_{y,67}}{10}\right) = c_{7,7}\left(\frac{K_{m,4}}{50,000}\right)\left(\frac{v_7 - v_6}{2500}\right)$ (s8)

Table 2. Continued

j	i	z_j (m)	z_{ij} (m)		
6	5		100	$\left(\frac{\tau_{y,56}}{10}\right) = c_{7,6}\left(\frac{K_{m,4}}{50,000}\right)\left(\frac{v_6 - v_5}{2500}\right)$	(s8)
5	4		50	$\left(\frac{\tau_{y,45}}{10}\right) = c_{7,5}\left(\frac{K_{m,4}}{50,000}\right)\left(\frac{v_5 - v_4}{2500}\right)$	
7	6		200	$\left(\frac{q_{c,67}}{.05}\right) = -c_{8,7}\left(\frac{K_{h,4}}{50,000}\right)\left(\frac{T_7 - T_6}{50}\right)$	
6	5		100	$\left(\frac{q_{c,65}}{.05}\right) = -c_{8,6}\left(\frac{K_{h,4}}{50,000}\right)\left(\frac{T_6 - T_5}{50}\right)$	(s9)
5	4		50	$\left(\frac{q_{c,54}}{.05}\right) = -c_{8,5}\left(\frac{K_{h,4}}{50,000}\right)\left(\frac{T_5 - T_4}{50}\right)$	
7	6		200	$\left(\frac{q_{e,67}}{.05}\right) = c_{9,7}\left(\frac{K_{v,4}}{50,000}\right)\left[c_{10,7}\left(\frac{e_6}{100}\right) - \left(\frac{e_7}{100}\right)\right]$	
6	5		100	$\left(\frac{q_{e,56}}{.05}\right) = c_{9,6}\left(\frac{K_{v,4}}{50,000}\right)\left[c_{10,6}\left(\frac{e_5}{100}\right) - \left(\frac{e_6}{100}\right)\right]$	(s10)

Table 2. Continued

j	i	z_j (m)	z_{ij} (m)		
5	4		50	$\left(\frac{q_{e,45}}{.05}\right) = c_{9,5}\left(\frac{K_{v,4}}{50,000}\right)\left[c_{10,5}\left(\frac{e_4}{100}\right) - \left(\frac{e_5}{100}\right)\right]$	(s10)
7	6		200	$K_{m,67} = b'_{67}\, K_{m,4}$	
6	5		100	$K_{m,56} = b'_{56}\, K_{m,4}$	
5	4		50	$K_{m,45} = b'_{45}\, K_{m,4}$	(s15)
7 6 5		250 150 75		$\left(\Delta g \frac{\partial h}{\partial x}\right)_j = \left[c_{11,j}\left(\frac{\partial T}{\partial x}\right)_4 + c_{12,j}\left(\frac{\partial T}{\partial x}\right)_7\right]$	(s17)
7 6 5		250 150 75		$\left(\Delta g \frac{\partial h}{\partial y}\right)_j = \left[c_{11,j}\left(\frac{\partial T}{\partial y}\right)_4 + c_{12,j}\left(\frac{\partial T}{\partial y}\right)_7\right]$	(s18)
		0		$\frac{\left(g \frac{\partial h}{\partial x}\right)_o}{1.736} = \frac{g \times 10^{-3}}{1.736}\left[\frac{ICG \sin (ICG)}{100} + \int\left(\frac{FCG \sin (FCG)}{100} - \frac{ICG \sin (ICG)}{100}\right)\frac{1440}{\Delta t}\right] dt$	(s23)

Table 2. Continued

j	i	z_j (m)	z_{ij} (m)	
		0		$\frac{\left(g\frac{\partial h}{\partial y}\right)_o}{1.736} = \frac{g \times 10^{-3}}{1\ 736}\left[\frac{ICG \cos (ICG)}{100} + \int\left(\frac{FCG \cos (FCG)}{100} - \frac{ICG \cos (ICG)}{100}\right)\frac{1440}{\Delta t}\right] dt$ (s24)
j	i	z_j (m)	z_{ij} (m)	B. Free air - canopy section, z = d
d		40		$\frac{R_N}{.05} = \left(\frac{q_{c,d+}}{.05}\right) + \left(\frac{q_{e,d+}}{.05}\right) + \left(\frac{q_{c,d-}}{.05}\right) + \left(\frac{q_{e,d-}}{.05}\right)$ (s19)
d		40		$\frac{R_N}{.05} = \frac{S_d}{.05} + \left(\frac{\sigma T_4^4}{.05}\right)\left(m + 10n\sqrt{\frac{e'_4}{100}}\right) - \varepsilon\left(\frac{\sigma T_d^4}{.05}\right)$ (s20)
d		40		$\frac{S_d}{.05} = \frac{I}{.05}(1 - J)\,\psi\, e^{-N} F_c \cos\zeta$ (s21)
d		40		$\frac{\cos\zeta}{1} = \frac{\sin\phi}{1}\frac{\sin\delta}{1} + \frac{\cos\phi}{1}\frac{\cos\delta}{1}\frac{\cos(15[t-12])}{1}$ (s22)
d		40		$\left(\frac{q_{c,d+}}{.05}\right) = c'_{8,4}\left(\frac{K_{h,4}}{50,000}\right)\left(\frac{T_d - T_4}{50}\right)$ (s25)

Table 2. Continued

j	i	z_j (m)	z_{ij} (m)		
d		40		$\left(\frac{q_{c,d-}}{.05}\right) = c'_{8,d}\left(\frac{K_{h,4}}{50,000}\right)\left(\frac{T_d - T_3}{.05}\right)$	(s26)
d		40		$\left(\frac{q_{e,d+}}{.05}\right) = c'_{9,4}\left(\frac{K_{v,4}}{50,000}\right)\left[\left(\frac{e_d}{100}\right) - \left(\frac{e_4}{100}\right)\right]$	(s27)
d		40		$\left(\frac{q_{e,d-}}{.05}\right) = c'_{9,d}\left(\frac{K_{v,4}}{50,000}\right)\left(\frac{e_d}{100} - \frac{e_3}{100}\right)$	(s28)
d		40		$\left(\frac{e_d}{100}\right) = \frac{e_{d,s}}{100} - \frac{.0005}{\xi}\left(\frac{q_{e,d+}}{.05}\right)$ $\quad q_{e,d+} \geq 0$	(s29)
d		40		$\left(\frac{e_d}{100}\right) = \frac{e_{d,s}}{100}$ $\quad q_{e,d+} \geq 0$	(s30)
d		40		$\left(\frac{e_{d,s}}{100}\right) = .0611 \times 10^{\iota}$; $\quad \iota = \frac{7.5T''_d}{237.3 + T''_d}$	(s31)
4	3		40	$\left(\frac{\tau_{x,d}}{10}\right) = c'_{7,4}\left(\frac{K_{m,4}}{50,000}\right)\left[\frac{u_4}{2500} - \left(\frac{1}{2.5}\right)\frac{u_3}{1000}\right]$	(s32)

Table 2. Continued

j	i	z_j (m)	z_{ij} (m)	
4	3		40	$\left(\frac{\tau_{v,d}}{10}\right) = c_{7,4}\left(\frac{K_{m,4}}{50,000}\right)\left[\frac{v_4}{2500} - \left(\frac{1}{2.5}\right)\frac{v_3}{1000}\right]$ (s33)
		45		$\frac{S_4}{2000} = \frac{(u_4^2 + v_4^2)^{1/2}}{2000}$ (s34)
		45		$\frac{Ri_4}{1} = \frac{50}{(2000)^2}\frac{\Delta g}{\theta}\left(\frac{\theta_4 - \theta_d}{50}\right)\frac{1}{\frac{(S_4 + 300)^2}{4 \times 10^6}}$ (s35)
		45		$\frac{\beta_4}{1} = 1.003 - 1.163\frac{Ri_4}{1} - 9.627\frac{Ri_4^2}{1}$ (s36)
		45		$\frac{K_{m,4}}{50,000} = \frac{(40)(2500)}{50,000}\left(\frac{\beta_{\kappa,4}}{40}\right)\left(\frac{S_4}{2500}\right)$, where $\beta_{\kappa,4} = \frac{k^2(1-\beta_4)z_{o,d}^{(1-\beta_4)}z^{\beta_4}}{\left(\frac{\Delta}{z_{o,d}}\right)^{1-\beta_4} - 1}$ (s37)

Table 2. Continued

j	i	z_j (m)	z_{ij} (m)	C. Forest, $\Lambda' < z < d-\Lambda$
3		35		$1440\left(\frac{u_3}{1000}\right) = \int \left[- \left(\frac{g\left(\frac{\partial h}{\partial x}\right)_o}{.6944}\right) + c_1\left(\frac{v_3}{1000}\right) + 5\, c_{2,3}\left(\frac{\tau_{x,d} - \tau_{x,23}}{10}\right) - \left(\frac{\alpha'_3 u_3 - \beta'_3 v_3}{.6944}\right) - c_{13} C'_{D,3}\left(\frac{u_3}{2500}\right)^2 \right] dt$ (slf)
2		15		$1440\left(\frac{u_2}{1000}\right) = \int \left[- \left(\frac{g\left(\frac{\partial h}{\partial x}\right)_o}{.6944}\right) + c_1\left(\frac{v_2}{1000}\right) + 5\, c_{2,2}\left(\frac{\tau_{x,23} - \tau_{x,12}}{10}\right) - c'_{3,2}\left(\frac{\alpha'_1 u_1 - \beta'_1 v_1}{.6944}\right) - c'_{4,2}\left(\frac{\alpha'_3 u_3 - \beta'_3 v_3}{.6944}\right) - c_{13} C'_{D,2}\left(\frac{u_2}{2500}\right)^2 \right] dt$
1		1.5		$1440\left(\frac{u_1}{1000}\right) = \int \left[- \left(\frac{g\left(\frac{\partial h}{\partial x}\right)_o}{.6944}\right) + c_1\left(\frac{v_1}{1000}\right) + 5\, c_{2,1}\left(\frac{\tau_{x,12} - \tau_{x,o}}{10}\right) - \left(\frac{\alpha'_1 u_1 - \beta'_1 v_1}{.6944}\right) - c_{13} C'_{D,1}\left(\frac{u_1}{2500}\right)^2 \right] dt$

Table 2, Continued

j	i	z_j (m)	z_{ij} (m)	
3		35		$1440\left(\frac{v_3}{1000}\right) = \int \left[- \left(\frac{g\left(\frac{\partial h}{\partial y}\right)_o}{.6944}\right) - c_1\left(\frac{u_3}{1000}\right) + 5\, c_{2,3}\left(\frac{\tau_{y,d} - \tau_{y,23}}{10}\right) - \left(\frac{\alpha'_3 v_3 + \beta'_3 u_3}{.6944}\right) - c_{13}\, C'_{D,3}\left(\frac{v_3}{2500}\right)^2 \right] dt$ (s2f)
2		15		$1440\left(\frac{v_2}{1000}\right) = \int \left[- \left(\frac{g\left(\frac{\partial h}{\partial y}\right)_o}{.6944}\right) - c_1\left(\frac{u_2}{1000}\right) + 5\, c_{2,2}\left(\frac{\tau_{y,23} - \tau_{y,12}}{10}\right) - c'_{3,2}\left(\frac{\alpha'_1 v_1 + \beta'_1 u_1}{.6944}\right) - c'_{4,2}\left(\frac{\alpha'_3 v_3 + \beta'_3 u_3}{.6944}\right) - c_{13}\, C'_{D,2}\left(\frac{v_2}{2500}\right)^2 \right] dt$
1		1.5		$1440\left(\frac{v_1}{1000}\right) = \int \left[- \left(\frac{g\left(\frac{\partial h}{\partial y}\right)_o}{.6944}\right) - c_1\left(\frac{u_1}{1000}\right) + 5\, c_{2,1}\left(\frac{\tau_{y,12} - \tau_{y,o}}{10}\right) - \left(\frac{\alpha'_1 v_1 + \beta'_1 u_1}{.6944}\right) - c_{13}\, C'_{D,1}\left(\frac{v_1}{2500}\right)^2 \right] dt$

Table 2. Continued

j	i	z_j (m)	z_{ij} (m)	
3		35		$1440\left(\frac{T_3}{50}\right) = \int \left[\frac{R}{.03472} - c_{5,3}\left(\frac{-q_{c,d-} - q_{c,23}}{.05}\right) - \left(\frac{u_3\left(\frac{\partial T}{\partial x}\right)_3 + v_3\left(\frac{\partial T}{\partial y}\right)_3}{.03472}\right) \right] dt$
2		15		$1440\left(\frac{T_2}{50}\right) = \int \left[\frac{R}{.03472} - c_{5,2}\left(\frac{q_{c,23} - q_{c,12}}{.05}\right) - c'_{3,2}\left(\frac{u_1\left(\frac{\partial T}{\partial x}\right)_1 + v_1\left(\frac{\partial T}{\partial y}\right)_1}{.03472}\right) - c'_{4,2}\left(\frac{u_3\left(\frac{\partial T}{\partial x}\right)_3 + v_3\left(\frac{\partial T}{\partial y}\right)_3}{.03472}\right) \right] dt$ (s3f)
1		1.5		$1440\left(\frac{T_1}{50}\right) = \int \left[\frac{R}{.03472} - c_{5,1}\left(\frac{q_{c,12} - q_{c,o}}{.05}\right) - \left(\frac{u_1\left(\frac{\partial T}{\partial x}\right)_1 + v_1\left(\frac{\partial T}{\partial y}\right)_1}{.03472}\right) \right] dt$
3		35		$1440\left(\frac{e_3}{100}\right) = \int \left[\frac{M}{.06944} - c_{6,3}\left(\frac{-q_{e,d-} - q_{e,23}}{.05}\right) - \left(\frac{u_3\left(\frac{\partial e}{\partial x}\right)_3 + v_3\left(\frac{\partial e}{\partial y}\right)_3}{.06944}\right) \right] dt$ (s4f)

Table 2. Continued

j	i	z_j (m)	z_{ij} (m)	
2		15		$1440\left(\frac{e_2}{100}\right) = \int\left[\frac{M}{.06944} - c_{6,2}\left(\frac{q_{e,23} - q_{e,12}}{.05}\right) - c'_{3,2}\left(\frac{u_1\left(\frac{\partial e}{\partial x}\right)_1 + v_1\left(\frac{\partial e}{\partial y}\right)_1}{.06944}\right) - c'_{4,2}\left(\frac{u_3\left(\frac{\partial e}{\partial x}\right)_3 + v_3\left(\frac{\partial e}{\partial y}\right)_3}{.06944}\right)\right] dt$ (s4f)
1		1.5		$1440\left(\frac{e_1}{100}\right) = \int\left[\frac{M}{.06944} - c_{6,2}\left(\frac{q_{e,12} - q_{e,0}}{.05}\right) - \left(\frac{u_1\left(\frac{\partial e}{\partial x}\right)_1 + v_1\left(\frac{\partial e}{\partial y}\right)_1}{.06944}\right)\right] dt$	
3	2		30	$\left(\frac{\tau_{x,23}}{20}\right) = c_{14,3}\left(\frac{u_3 - u_2}{1000}\right)\left(\frac{c'_{3,3}\ K_{m,1} + c'_{4,3}\ K_{m,4}}{50,000}\right)$
2	1		3	$\left(\frac{\tau_{x,12}}{20}\right) = c_{14,2}\left(\frac{u_2 - u_1}{1000}\right)\left(\frac{c'_{3,2}\ K_{m,1} + c'_{4,2}\ K_{m,4}}{50,000}\right)$ (s7f)

Table 2. Continued

j	i	z_j (m)	z_{ij} (m)		
3	2		30	$\left(\frac{\tau_{y,23}}{20}\right) = c_{14,3}\left(\frac{v_3 - v_2}{1000}\right)\left(\frac{c'_{3,3} K_{m,1} + c'_{4,3} K_{m,4}}{50,000}\right)$	(s8f)
2	1		3	$\left(\frac{\tau_{y,12}}{20}\right) = c_{14,2}\left(\frac{v_2 - v_1}{1000}\right)\left(\frac{c'_{3,2} K_{m,1} + c'_{4,2} K_{m,4}}{50,000}\right)$	
		0		$\left(\frac{u_{geo}}{2500}\right) = -\frac{1}{2\omega \sin \phi} \frac{\rho\left(\frac{\partial h}{\partial y}\right)_o}{1.736}$	(s9f)
		0		$\left(\frac{v_{geo}}{2500}\right) = \frac{1}{2\omega \sin \phi} \frac{g\left(\frac{\partial h}{\partial x}\right)_o}{1.736}$	(s10f)
3	2		30	$\left(\frac{q_{c,23}}{.05}\right) = -c_{15,3}\left(\frac{T_3 - T_2}{50}\right)\left(\frac{c'_{3,3} K_{h,1} + c'_{4,3} K_{h,4}}{50,000}\right)$	(s11f)
2	1		3	$\left(\frac{q_{c,12}}{.05}\right) = -c_{15,2}\left(\frac{T_2 - T_1}{50}\right)\left(\frac{c'_{3,2} K_{h,1} + c'_{4,2} K_{h,4}}{50,000}\right)$	

Table 2. Continued

j	i	z_j (m)	z_{ij} (m)	
3	2		30	$\left(\frac{q_{e,23}}{.05}\right) = c_{16,3}\left[c_{10,3}\left(\frac{e_3}{100}\right) - \frac{e_3}{100}\right]\left(\frac{c'_{3,3}\,K_{v,1} + c'_{4,3}\,K_{v,4}}{50,000}\right)$
2	1		3	$\left(\frac{q_{e,12}}{.05}\right) = c_{16,2}\left[c_{10,2}\left(\frac{e_2}{100}\right) - \frac{e_1}{100}\right]\left(\frac{c'_{3,2}\,K_{v,1} + c'_{4,2}\,K_{v,4}}{50,000}\right)$ (s12f)
3	2		30	$K_{m,23} = c'_{3,3}K_{m,1} + c'_{4,3}K_{m,4}$
2	1		3	$K_{m,12} = c'_{3,2}K_{m,1} + c'_{4,2}K_{m,4}$ (s17f)
j	i	z_j (m)	z_{ij} (m)	D. Forest surface section, z = 0
		0		$\frac{R_N}{.05} = \left(\frac{q_{c,o}}{.05}\right) + \left(\frac{q_{e,o}}{.05}\right) + \left(\frac{q_{s,o}}{.05}\right)$ (s18f)
		0		$\frac{R_N}{.05} = \chi S_d + \left(\frac{\sigma T'^4_{A,}}{.05}\right)\left(m + 10n\sqrt{\frac{e'_{A,}}{100}}\right) - \varepsilon\left(\frac{T_o^4}{.05}\right)$ (s19f)*

* Equations s20f through s23f have been combined with equation s19f and do not appear explicitly in this report. These equation numbers have been retained in order to maintain consistency with equation numbers in previous reports.

Table 2. Continued

j	i	z_j (m)	z_{ij} (m)		
		0		$\frac{e_o}{100} = \frac{e_{o,s}}{100} - \frac{.05}{s_o}\left(\frac{q_{e,o}}{.05}\right)$; $q_{e,o} > 0$	(s24f)
		0		$\frac{e_o}{100} = \frac{e_{o,s}}{100}$; $q_{e,o} \leq 0$	(s25f)
		0		$\frac{T'_o}{50} = \frac{T_o}{50} - \left(\frac{G}{5000}\right)\left(\frac{q_{s,o}}{.01}\right)$	(s26f)
		0		$\frac{q_{e,o}}{.05} = \frac{(1000)\rho a \bar{L}}{.05 p_o}\left(\frac{D_1}{10}\right)\left(\frac{e_o - e_1}{100}\right)$	(s27f)
		0		$\frac{q_{c,o}}{.05} = \frac{(500)\rho C_p}{.05}\left(\frac{D_1}{10}\right)\left(\frac{T_o - T_1}{50}\right)$	(s28f)
		0		$1440\left(\frac{T'_o}{50}\right) = \int \left[\frac{(1440)(.05)}{50} 2\sqrt{\frac{\pi}{P\mu\lambda}}\left(\frac{q_{s,o}}{50}\right) - \frac{2\pi}{P}\left(\frac{T'_o - T'_s}{50}\right)\right] dt$	(s29f)
		0		$\frac{\tau_{x,o}}{10} = \frac{(10)(1000)}{10}\rho\left(\frac{D_1}{10}\right)\left(\frac{u_1}{1000}\right)$	(s30f)

Table 2. Continued

j	i	z_j (m)	z_{ij} (m)	
		0		$\frac{\tau_{y,o}}{10} = \frac{(10)(1000)}{10} \rho \left(\frac{D_1}{10}\right)\left(\frac{v_1}{1000}\right)$ (s31f)
		0		$\frac{e_{o,s}}{100} = 0.0611 \times 10^{\iota} \quad ; \quad \iota = \frac{7.5T''_o}{237.3 + T''_o}$ (s32f)
		1.5		$\frac{S_1}{1000} = \frac{\left[u_1^2 + v_1^2\right]^{1/2}}{1000}$ (s33f)
		1.5		$\frac{Ri_1}{1} = \frac{50}{(1000)^2} \frac{\Lambda' g}{\theta} \left(\frac{\theta_1 - \theta_o}{50}\right) \frac{1}{\left(\frac{S_1 + 300}{1000}\right)^2}$ (s34f)
		1.5		$\frac{\beta_1}{1} = 1.003 - 1.163 \frac{Ri_1}{1} - 9.627 \frac{Ri_1^2}{i}$ (s35f)
		1.5		$\frac{D_1}{10} = \frac{(.006)(1000)}{10} \left(\frac{\beta_\delta}{.006}\right)\left(\frac{S_1}{1000}\right)$, where $\beta_\delta = \left[\frac{k(1-\beta_1)}{\left(\frac{\Lambda'}{z_o}\right)^{1-\beta_1} - 1}\right]^2$ (s36f)

Table 2. Continued

j	i	z_j (m)	z_{ij} (m)	
		1.5		$\frac{K_{m,1}}{50,000} = \frac{(40)(1000)}{50,000}\left(\frac{\beta_{\kappa,1}}{40}\right)\left(\frac{S_1}{1000}\right)$, where $\beta_{\kappa,1} = \frac{k^2(1-\beta_1)z_o^{(1-\beta_1)}z^{\beta_1}}{\left[\left(\frac{\Lambda'}{z_o}\right)^{1-\beta_1} - 1\right]}$ (a37f)

Table 3. Form and numerical values of the coefficients, c, in the scaled equations.

Coefficient	j = 1	2	3	4	5	6	7
$b'_{i,j} = \frac{K_{m,ij}}{K_{m,4}}$, $4 \le j \le 7$ (eqn. a 16)	—	—	—	1.0000	1.9809	10.7701	23.2112
$c_1 = 1440\ (2\omega)\ \sin\phi$	.2101 sin ϕ						
$c_{2,j} = \frac{1440}{2500}\left(\frac{10}{\rho\ \Delta z_j}\right)$; $c'_{2,7} = c_{2,7}\left(\frac{K_{m,78}}{K_{m,67}} - 1\right)$	16.0000	1.7778	4.8000	4.8000	.9600	.4800	.1344
$c_{3,j} = (1 - c_{4,j})$; $c'_{3,j} = (1 - c'_{4,j})$	1.0000	.5970	.0000	1.0000	.8537	.4878	.0000
$c_{4,j} = \frac{z_j - z_4}{z_7 - z_4}$, $7 \le j \le 4$; $c'_{4,j} = \frac{z_j - z_1}{z_3 - z_1}$, $3 \le j \le 1$	.0000	.4030	1.0000	.0000	.1463	.5122	1.0000
$c_{5,j} = \frac{1440}{50}\left(\frac{.05}{\rho C_p \Delta z_j}\right)$; $c'_{5,7} = c_{5,7}\left(\frac{K_{m,78}}{K_{m,67}} - 1\right)$	16.667	1.8519	5.0000	5.0000	1.0000	.5000	.1402
$c_{6,j} = \frac{1440}{100}\left(\frac{.05p_j}{\rho g L \Delta z_j}\right)$; $c'_{6,7} = c_{6,7}\left(\frac{K_{m,78}}{K_{m,67}} - 1\right)$	5.4932	.6093	1.6413	1.6394	.3267	.1619	.0449
$c_{7,j} = \frac{(50,000)(2500)\rho}{10(z_j - z_1)}\left(\frac{K_{m,ij}}{K_{m,4}}\right)$; $j > 4$	—	—	—	—	9.9047	21.5402	34.8168
$c'_{7,4} = \frac{(50,000)(2500)\rho}{10 z_d (\ell n\ z_4 - \ell n\ z_3)}$	—	—	—	14.9216	—	—	—
$c_{8,j} = \frac{(50,000)(50)\rho C_p}{.05(z_j - z_1)}\left(\frac{K_{m,ij}}{K_{m,4}}\right)$; $j > 4$	—	—	—	—	9.5064	20.6776	33.4221

Table 3. Continued

Coefficient	1	2	3	4	5	6	7
$c'_{8,j} = \frac{(50,000)(50)\rho C_p}{.05\lvert z_j - z_d\rvert}$, $j = 4$	—	—	—	28.8000	—	—	—
$c_{9,j} = \frac{(50,000)(100)\rho aL}{.05\ p_j(z_j - z_i)}\left(\frac{K_{m,ij}}{K_{m,4}}\right)$, $j > 4$	—	—	—	—	29.0952	63.8472	104.4349
$c'_{9,j} = \frac{(50,000)(100)\rho aL}{.05\ p_d\lvert z_j - z_d\rvert}$; $j = 4$	—	—	—	87.7850	—	—	—
$c_{10,j} = \frac{p_j}{p_i}$	1.0000	.9984	.9977	—	.9965	.9912	.9882
$c_{11,j}$	—	—	—	—	.1356	.3810	.5000
$c_{12,j}$	—	—	—	—	.0107	.1312	.5000
$c_{13,j} = \frac{1}{2}(1440)(1000)^2$	7.2×10^8	7.2×10^8	7.2×10^8	7.2×10^8	7.2×10^8	7.2×10^8	7.2×10^8
$c_{14,j} = \frac{(5000)(1000)\rho}{(10)(z_j - z_i)}$; $1 < j \leq 3$	—	.4444	.3000	—	—	—	—
$c_{15,j} = \frac{(50,000)(50)\rho C_p}{.05\ (z_j - z_i)}$; $1 < j \leq 3$	—	10.6667	7.2000	—	—	—	—
$c_{16,j} = \frac{(50,000)(100)\rho aL}{.05\ p_j(z_j - z_i)}$; $1 < j \leq 3$	—	32.3624	21.8451	—	—	—	—

time scale factor of 1440. The scale factor for $\Delta(g\partial h/\partial x)$ is shown to be 1.736. This is the wind scale factor of 2500 divided by a time scale factor of 1440. The advection terms $(\alpha'_7 u_7 - \beta'_7 v_7)$ also are shown to be scaled over 1.736. The first term on the right hand side of the equation is written as $.4g(\partial h/\partial x)/.6944$. This term is written in this manner to show the one to one correspondence between the equation format and the calculation of this term in the analog computer solution diagrams. In the solution diagrams, $g(\partial h/\partial x)_0/.6944$ is calculated and then multiplied by .4 to obtain a scale value for the pressure gradient term of 1.736.

The north-south component of wind in the Coriolis term is scaled for a maximum value of 2500 cm/sec. The coefficient c_1 is shown in Table 3 to be 1440 (2ω) sin ϕ and applies at each atmospheric height. In addition, the east-west component of the shearing stress of the wind is scaled for a maximum of 10 dynes/cm^2. The coefficient $c'_{2,7}$ is shown in Table 3 to consist of the time scale factor divided by the wind scale factor, multiplied by the scale factor for the shearing stress divided by air density and the thickness of the layer centered at 250 m, and further multiplied by the ratio of the momentum exchange coefficient at 300 m divided by the momentum exchange coefficient at 200 m minus one. The calculated values for each level, j, is shown in Table 3.

The equations in the set which are not solved explicitly on the General Purpose Analog Computer are listed in unscaled format in Table 4. These equations consist of equation (5) which describes the lapse of pressure with increasing height; equation (11) which relates

the specific humidity to the vapor pressure and the atmospheric pressure; equation (12) which expresses the rate of gain or loss of heat per unit mass to the system; equation (13) the equation of state for a perfect gas; and equation (14) which relates the vertical exchange coefficients for momentum heat and water vapor. Since these equations appear implicitly in the wiring diagrams, scaling is not required.

Two numbers, one of which is followed by the letter f (forest), are assigned to each equation. This double numbering has been done in order to point out the fact that the equations apply to both the free atmosphere above the forest and the atmosphere within the forest.

Table 4. Implicit relations in the solution diagrams.

$p = p_o - \rho g z$	(5) and (5f)
$r = ae/p$	(11) and (13f)
$R = \frac{1}{C_p} \frac{dQ}{dt}$	(12) and (14f)
$\rho = p/R_a T$	(13) and (15f)
$K_m = K_h = K_v$	(14) and (16f)

IV. Analog Solution Diagrams for Tropical Forest Simulation

There are many ways to solve the scaled equations on the analog computer. The methods employed depend upon many factors, but are primarily controlled by the quantity, quality, and nature of the available computing components. The method shown here is only one of many that could be employed and would be compatible with the available computing equipment.

Efforts have been made in setting up the solution diagrams to treat each parameter as a variable as far as is possible. The values of these variables may be easily changed from case to case, although for a particular case, the variable may be held constant during the solution period. Discussion of the diagrams on a one-to-one correspondence basis with the equations shown in Section III is not practical since there is considerable duplication of the wiring patterns due to the similarity of the equations for the individual layers; however, a brief explanation of the solution of each type of equation will assist the reader in making the correspondence for the solution of the individual equations for the various layers.

The symbols employed in the analog diagrams and their interpretation are shown in Table 5. The left-hand column of this table shows the symbol employed and the right-hand column indicates its interpretation.

The analog solution diagrams begin on page 30 on which the computer diagrams for the solution of the east-west wind components appear. This diagram is the programmed solution of equation (s1)

Table 5. Analog wiring symbols.

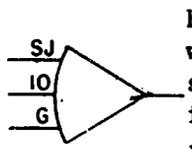

High gain amplifier with an input to the summing junction, an input resistor of .1 megohm, an input directly to the grid, and no feedback

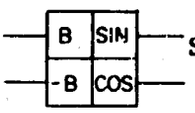

Servo resolver cup

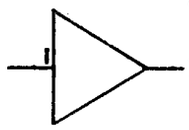

Inverter

Capacitor

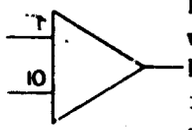

High gain amplifier with one megohm feedback resistor and inputs of 1.0 and .1 megohm (summer)

Variable function generator

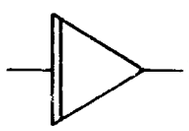

Integrator

Resistor

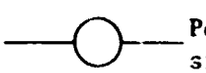

Potentiometer (low side grounded)

Diode

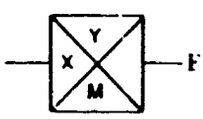

Electronic multiplier

Ground

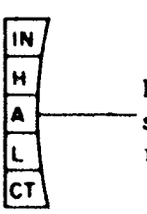

Follow-up cup of a servo multiplier or resolver

Function switch

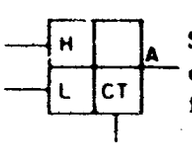

Servo multiplier cup (other than follow-up)

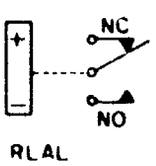

Low speed relay comparator

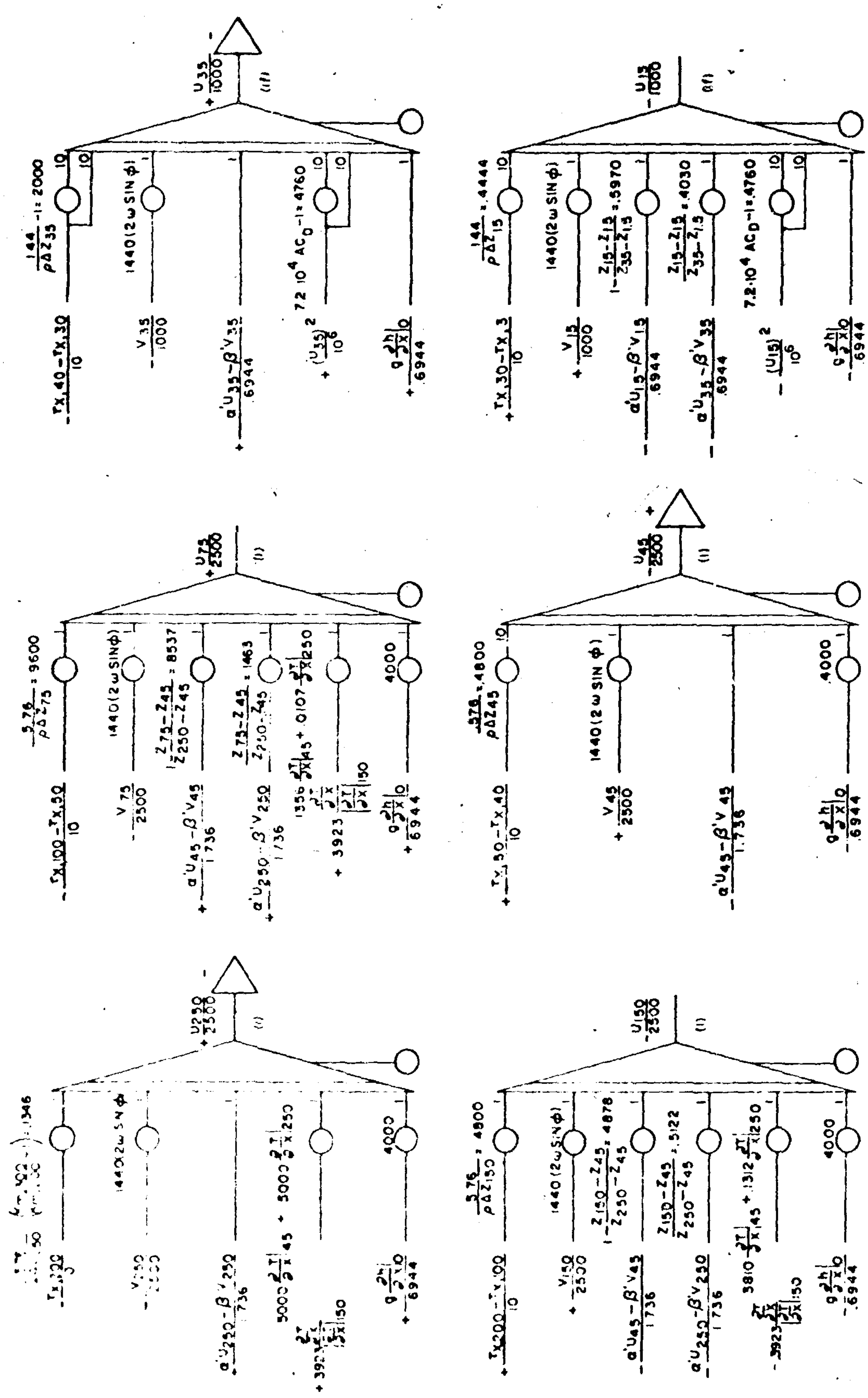

EAST - WEST COMPONENTS OF WIND

shown on page 5. The solution for the east-west component of the wind for the layer at 150-m height appears in the lower left-hand corner of page 30.

The east-west wind component $-u_{150}/2500$ is obtained as the output of an integrator which sums the individual terms appearing on the right-hand side of equation (s1). The initial condition of the east-west wind component at 150 m is obtained from observed values and is supplied to the integrator through the initial condition potentiometer. This potentiometer supplies the initial voltage from which the amplifier integrates. The remaining inputs are calculated in the following manner.

1. Vertical divergence of the shearing stress. The vertical divergence of the shearing stress is calculated from the winds at 75, 150, and 250 m. The solution diagram is shown in the upper center portion of page 32. Voltages representing $+u_{250}/2500$ and $-u_{150}/2500$ are applied individually to 10-gain inputs* of an amplifier having a potentiometer set to $(Z_{250} - Z_{150})\ K_{m,45}/1.25 \times 10^6\ \rho\ K_{m,250}$ as a feedback element to calculate $-(\tau_{x,200}/10)/(K_{m,45}/50,000)$. The output of this amplifier is multiplied by $+K_{m,45}/50,000$ by means of a servomultiplier. The product of these terms $-\tau_{x,200}/10$ is obtained from the arm of the servomultiplier and the east-west component of the shearing stress $+\tau_{x,100}/10$ is determined in an analogous manner from the next lower amplifier and servomultiplier. The terms $+\tau_{x,100}/10$ and

*All amplifiers employed in the solution diagrams are of the inverting type; therefore, the terms unity gain or 10 gain imply a sign change within the amplifier.

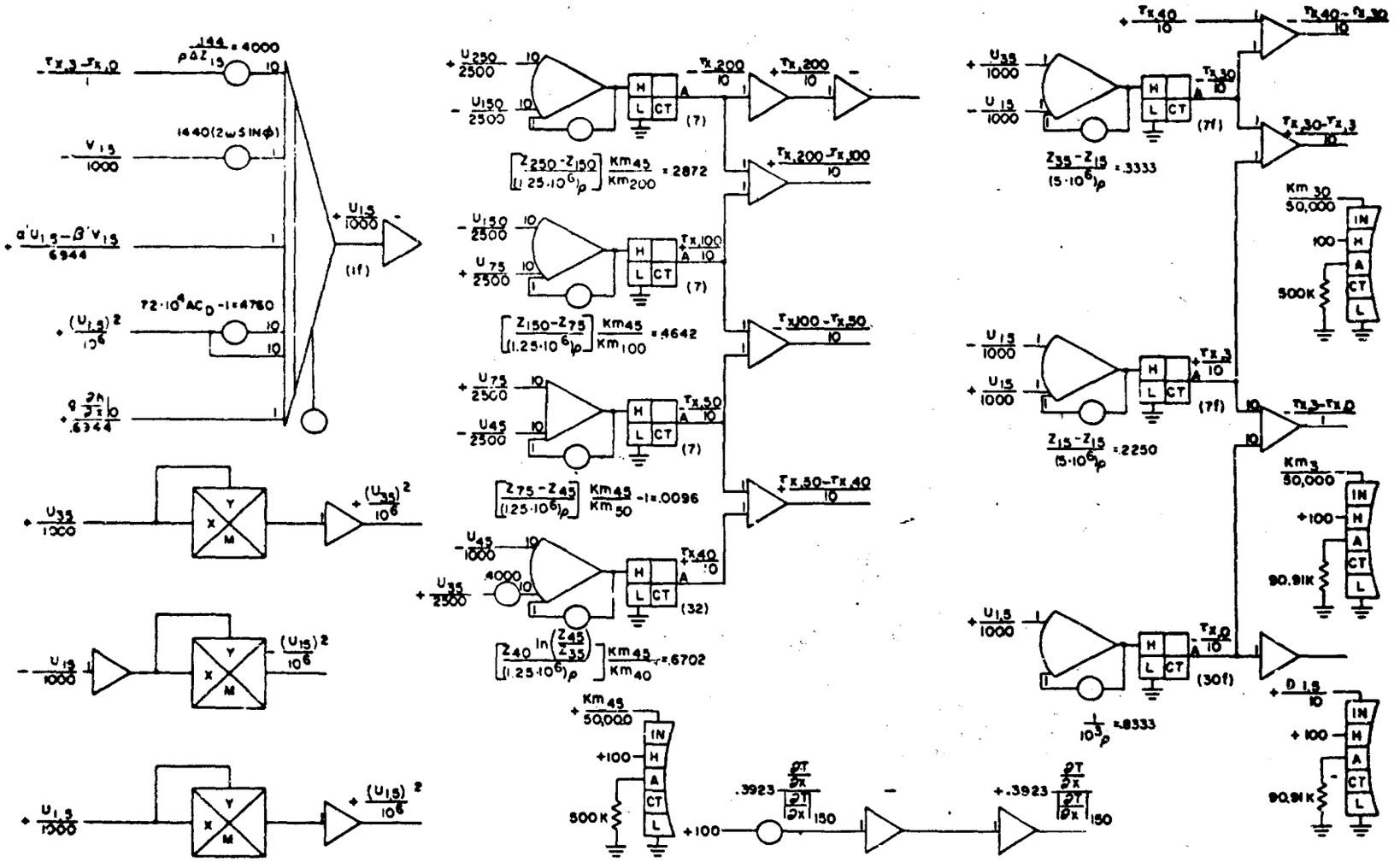

EAST — WEST COMPONENTS OF WIND STRESS

$-\tau_{x,200}/10$ are added in a summing amplifier to obtain the difference of the stresses at the two levels + $(\tau_{x,200} - \tau_{x,100})/10$. This difference is further multiplied by $5.76/\rho\ \Delta Z_{150}$ on a potentiometer and applied at a gain of one to the input of the $-u_{150}/2500$ integrator.

2. Coriolis term. The Coriolis term for the east-west component of the wind at 150 m is obtained by multiplying the north-south wind component at 150 m, calculated by the $-v_{150}/2500$ integrator on page 39 and inverted in sign by a unity gain amplifier, by 2880 $\omega \sin \phi$ on a potentiometer and applying the resultant voltage at a unity gain on the $-u_{150}/2500$ integrator.

3. Wind advection. Wind advection is calculated for the layers at heights of 1.5 m, 35 m, 45 m, and 250 m. Advection between these layers is obtained by linear interpolation. Advection of wind, temperature, and vapor pressure is handled in this manner. Since linear interpolation is used at 150 m height for advection, two inputs are required to the $-u_{150}/2500$ integrator. There is a contribution from the advection at both 45 m and 250 m, the calculation of which appears on page 34. Positive and negative values of the east-west and north-south wind components are applied independently to two function switches. The up position of the first function switch is connected to $+u_{250}/2500$ and the down position of the switch to $-u_{250}/2500$. The up position of the second function switch is connected to $-v_{250}/2500$ and the down position to $+v_{250}/2500$. The arm of the first function switch is connected to a potentiometer having a setting of 1440 α'_{250}; thus, the voltage appearing on the arm of this potentiometer represents $+1440\ \alpha'_{250}\ u_{250}/2500$ or $-1440\ \alpha'_{250}\ u_{250}/2500$ depending upon whether the

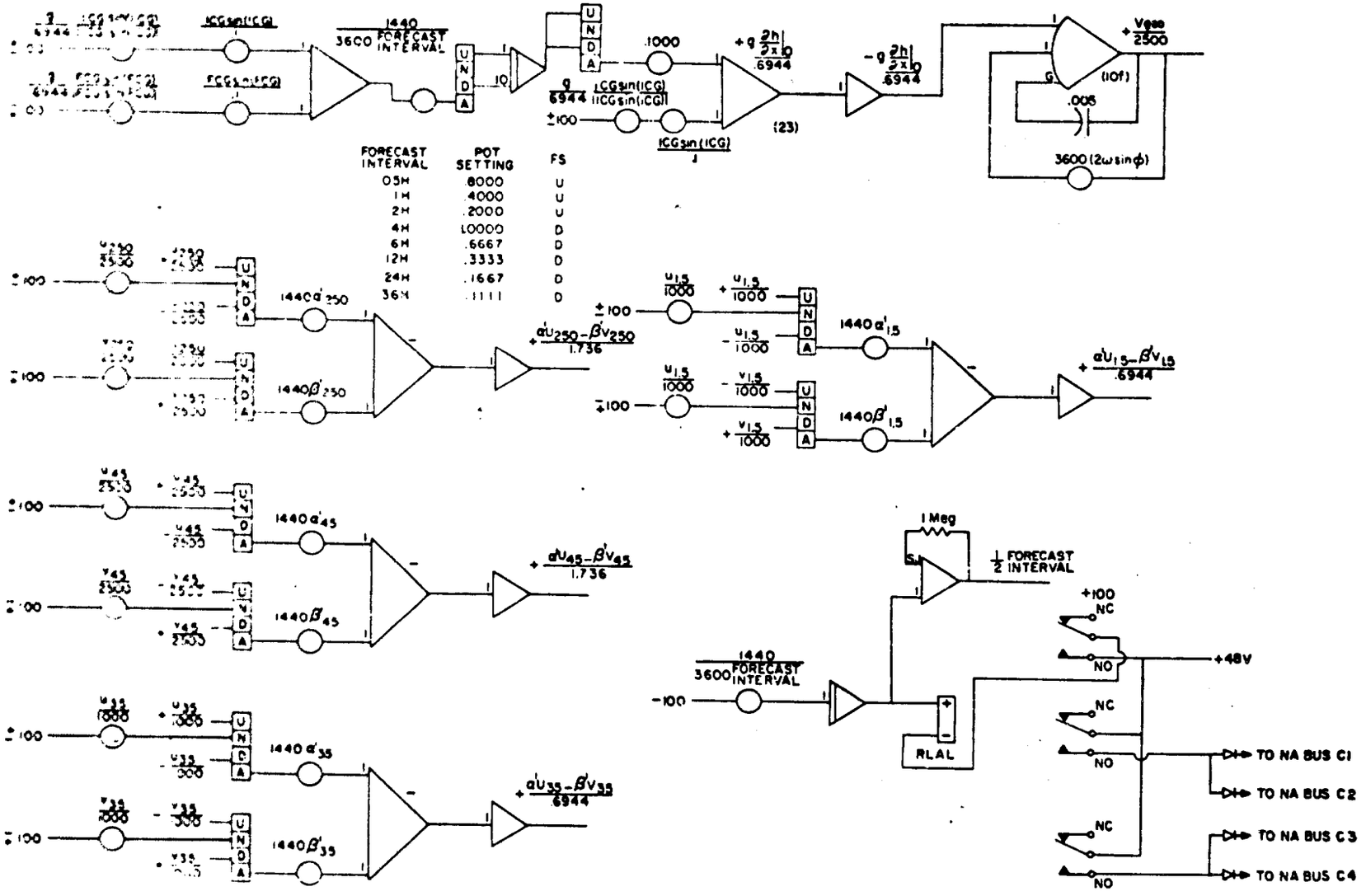

EAST–WEST COMPONENT OF THE SURFACE CONTOUR GRADIENT
AND ADVECTION OF EAST–WEST WINDS

function switch is in the up position or in the down position. Similarly, the up position of the second function switch calculates $-1440\ \beta'_{250}v_{250}/2500$ at the arm of the potentiometer connected to the arm of the second function switch. These two terms are added in a summing amplifier to obtain the advection at 250 m, $\pm(\alpha' u_{250} - \beta' v_{250})/1.736$.

The neutral positions of the function switches are wired individually to the arms of two potentiometers. The initial values of the winds are set on these potentiometers so that advection may be held constant at the initial value throughout the solution period. Whether advection is held fixed at the initial value or allowed to vary with wind speed, the gradients of the wind α' and β' are held constant throughout the solution period.

Advection at 45 m is determined in precisely the same manner as that at 250 m. These advection terms are multiplied by appropriate factors appearing on potentiometers of which the arms are connected to unity gain inputs on the $-u_{150}/2500$ integrator to provide linear interpolation between 45 m and 250 m height.

4. Surface height-contour gradient. The solution diagram for the gradient of the surface height contours is found at the top of page 34 for the east-west height-contour gradient. This solution diagram is the schematic representation of equation (s23) on page 11. A potentiometer, having the computer reference voltage applied to its high potential contact, is set to the value g ICG sin (ICG)/6944|ICG sin (ICG)|. This factor is multiplied by ICG sin (ICG) which is set on the second

of the series potentiometers. The arm of this second potentiometer has as an output the product $\pm g$ ICG sin (ICG)/6944. The sign of this product is determined by the ratio ICG sin (ICG)/|ICG sin (ICG)| which is included in the first potentiometer setting.

The product $\pm g$ FCG sin (FCG) is computed by the two series potentiometers which appear just below those for the initial contour gradient. These two values are added by a summing amplifier and multiplied by 1440/3600 FI, where FI is the prediction time interval expressed in hours, and applied to either a unity gain or 10-gain input of an integrator depending upon the setting of the potentiometer which supplies the integrator input voltage. If the potentiometer is set for a solution period greater than or equal to 4 hr, a gain of unity is selected by placing the function switch in the up position. For solution periods of less than 4 hr, a gain of 10 is selected.

The output of the integrator is the expression occurring under the integral sign of equation (s23) save a factor of .1000 which appears on the potentiometer following the integrator; thus, the arm of this potentiometer carries the value $1440\ g \int([\text{FCG sin (FCG)} - \text{ICG sin (ICG)}]/6944\ \Delta t)dt$, where Δt is in seconds. Two additional series potentiometers calculate $\pm g$ ICG sin (ICG)/6944. These two values are added by a summing amplifier to obtain $+g\ \partial h/\partial x|_o/.6944$. This solution procedure permits linear variation of the surface contour gradient with time. The potentiometer set to .1000 is used simply to allow higher input voltages to be applied to the integrator for long solution periods.

The east-west component of the surface contour gradient is inverted in sign by an amplifier and further applied to a high gain amplifier having a feedback potentiometer set to 3600 ($2\omega \sin \phi$); therefore, the gain of this amplifier is $1/7200\ \omega \sin \phi$ and the surface contour gradient is multiplied by this value to obtain the north-south component of the geostrophic wind.

The surface height-contour gradient, $-g(\partial h/\partial x)_0/.6944$, is further multiplied by .4000 set on a potentiometer, of which the arm is connected to a unity gain input of the $-u_{150}/2500$ integrator and which scales the surface height-contour gradient to the proper value of 1.736.

5. Variation of the contour gradient with height. The variation of the height-contour gradients with altitude depends upon the gradients of the mean virtual temperature within the layer under consideration. The computer program appears on page 32 in the lower right-hand corner. The voltage on a potentiometer set to $.3923\ (\partial T/\partial x)_{150}/|(\partial T/\partial x)_{150}|$ is applied to an inverting amplifier of which the output is connected to potentiometers having settings of $a(\partial T/\partial x)_{45} + b(\partial T/\partial x)_{250}$. The coefficients a and b have, respectively, the values .1356 and .0107 at 75-m height, .3810 and .1312 at 150-m height, and .5000 and .5000 at 250-m height. These values yield output voltages which represent $\Delta[g(\partial h/\partial x)_j]/1.736$ where j is the index of the layer in question. The surface contour gradient is assumed constant with height up through 45 m; therefore, this term is not applied at and below 45 m.

At the heights of 1.5, 15, and 35 m an additional input is applied to the integrators. This input represents the drag upon the air produced by trees and other foliage. The calculation of this drag

term is shown on page 40 and consists of the squaring of the wind component from the output of an amplifier by applying it to the x and y inputs of an electronic multiplier. This product is inverted in sign by use of an inverting amplifier and further applied to a gain of 10 and also multiplied by the coefficient $[(7.2 \times 10^4 AC_D)-1]$ which is set on a potentiometer the arm of which is connected to a gain of 10.

The circuit shown in the lower right-hand corner of page 34 is a timing circuit which automatically places the computer in HOLD mode at the termination of a computational cycle. In this mode the solutions are stored until they can be printed by a digital printer or placed on punch cards. As one can see from this diagram, +100 volts is connected to the normally closed contact of a relay. This voltage is applied to the arm of the first set of contacts on the relay and subsequently to the negative terminal of this relay, RLAL. The normally open contact is connected to +48 volts as are the arms of the remaining two sets of relay contacts. The output of an integrator is connected to the positive terminal of the relay. The input to the integrator is a potentiometer having a setting of 1440/3600 FI, where, FI is the solution interval in hours when the output of the integrator is less than +100 volts, which is the voltage applied to the negative contact of the relay, the relay coil remains unenergized and the contacts on the relay remain in the normally closed position; however, when the output voltage of the integrator exceeds +100 volts the relay is energized and the contacts are

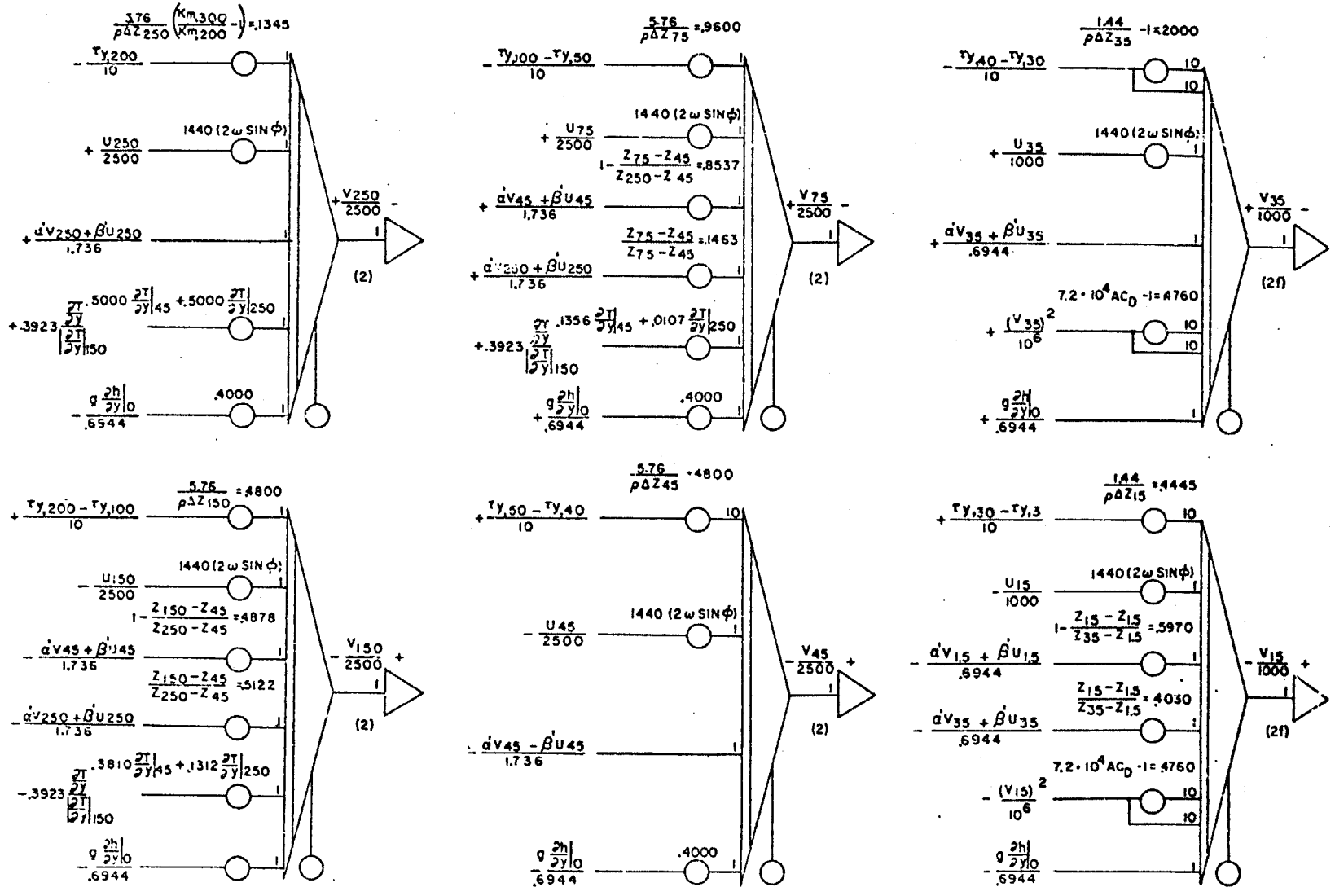

NORTH - SOUTH COMPONENTS OF WIND

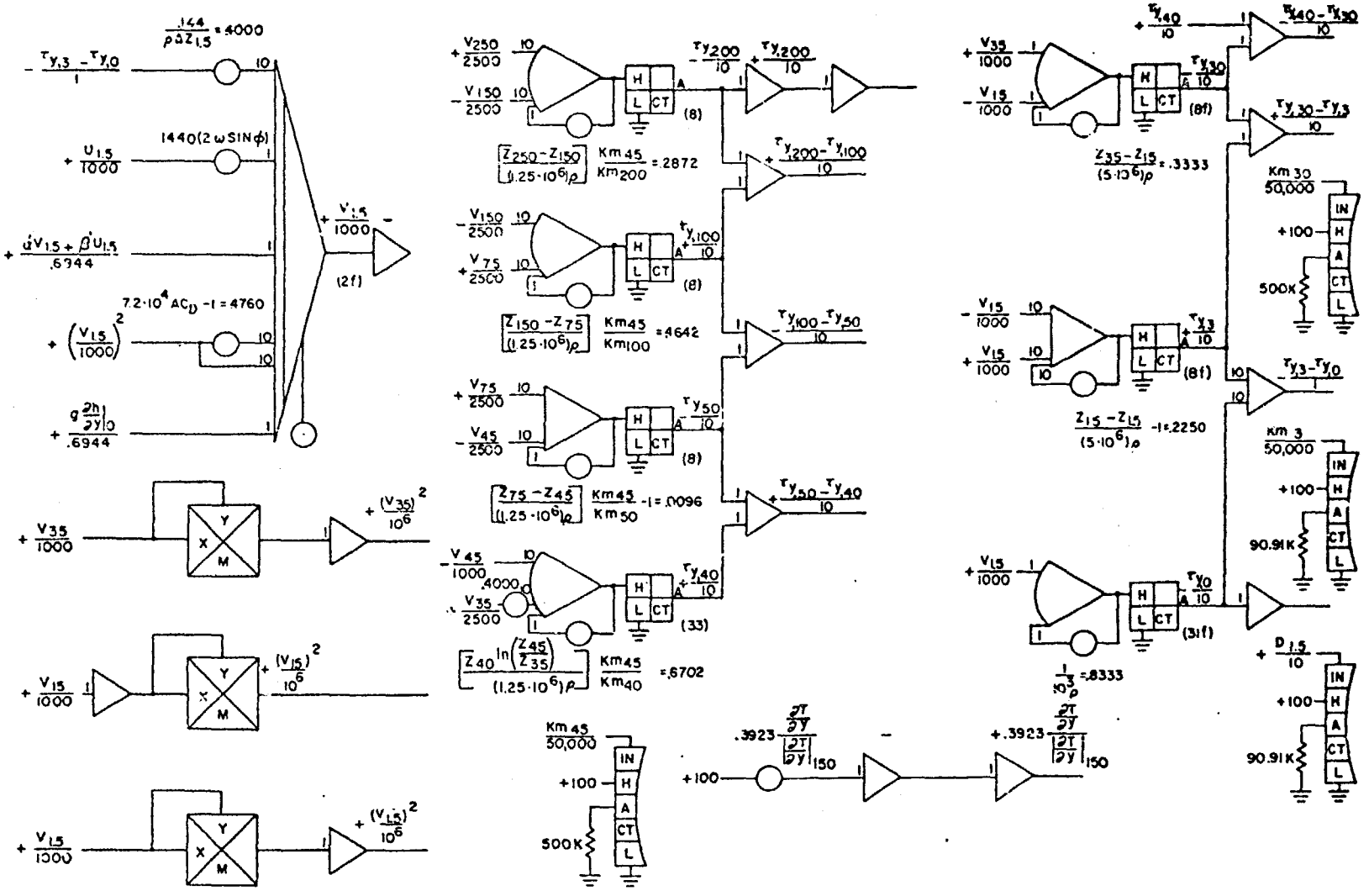
NORTH-SOUTH COMPONENTS OF WIND STRESS

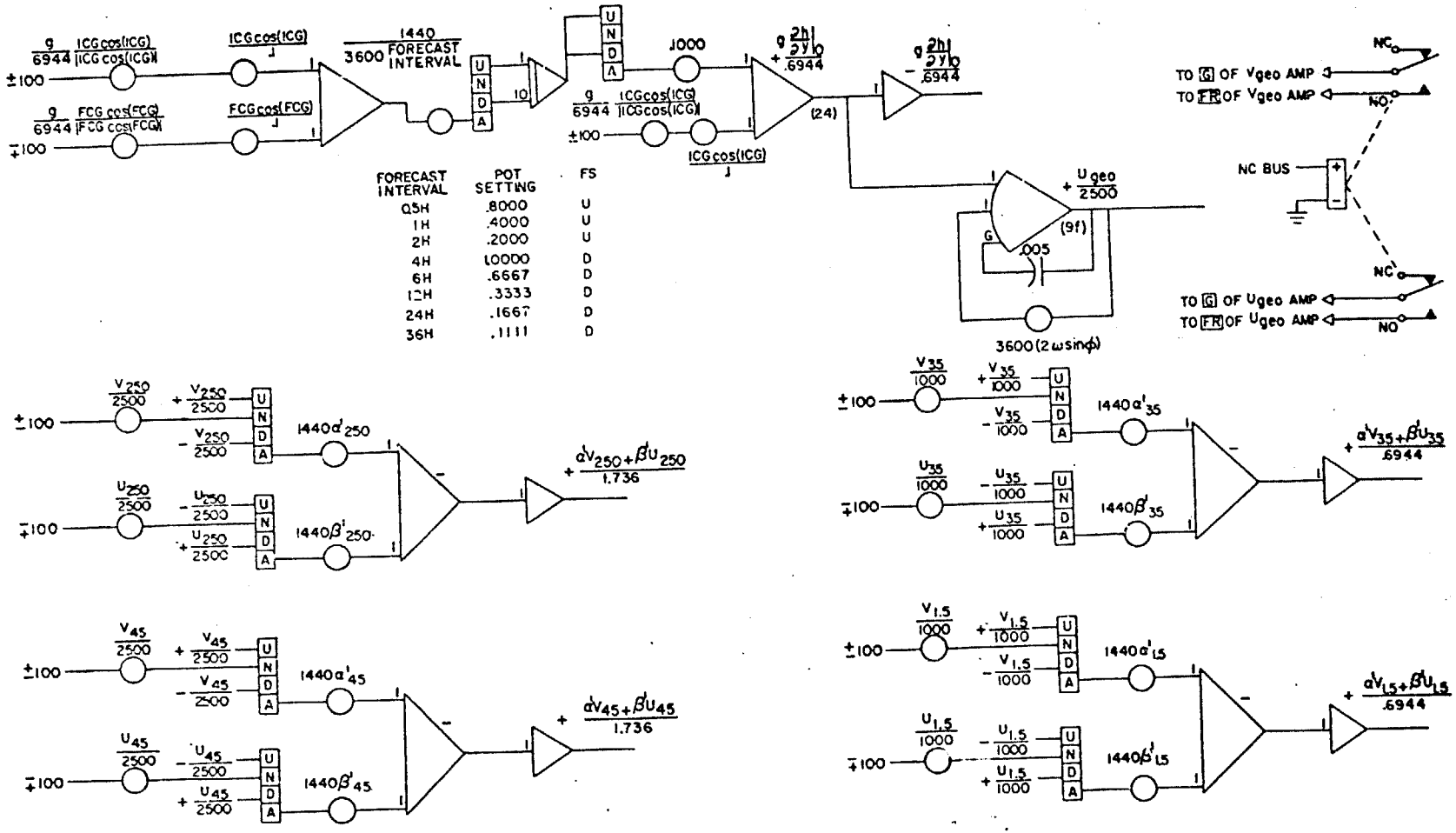

NORTH–SOUTH COMPONENT OF THE SURFACE CONTOUR GRADIENT
AND ADVECTION OF NORTH–SOUTH WINDS

switched to the normally open position. Under these conditions, +48 volts is connected to the negative side of the relay input. This arrangement provides a positive voltage differential of approximately +52 volts between the positive and negative relay inputs. This large differential in voltage assures a positive locking of the relay in the energized position and prevents relay chatter. Simultaneously, +48 volts is applied to the normally open contacts of the other two sets of relay contacts. This +48 volts is transferred to the NA bus of each console through isolating diodes in order to energize the hold relays which stop computation at the time specified by the setting of the potentiometer connected to the input of the timing integrator. The output of the timing integrator is applied to the input of a summing amplifier having a gain of 1/2. This 1/2-gain amplifier simply provides a convenient means for monitoring the time period for computer simulations.

The solution of the set of equations representing the energy balance at the top of the forest is shown on page 43 and consists of wiring diagrams for equations s19 through s37 excepting equations s23, s24, and s32 through s34. The solution diagram for the calculation of the cosine of the solar zenith angle, equation s22, is shown at the top of page 43. The solution diagram consists of a sine-cosine oscillator with initial conditions for the sine and cosine of the local hour angle, H. The cosine of the local hour angle is taken from the second integrator and multiplied by cos ϕ on a potentiometer. This product is further multiplied by cos δ which

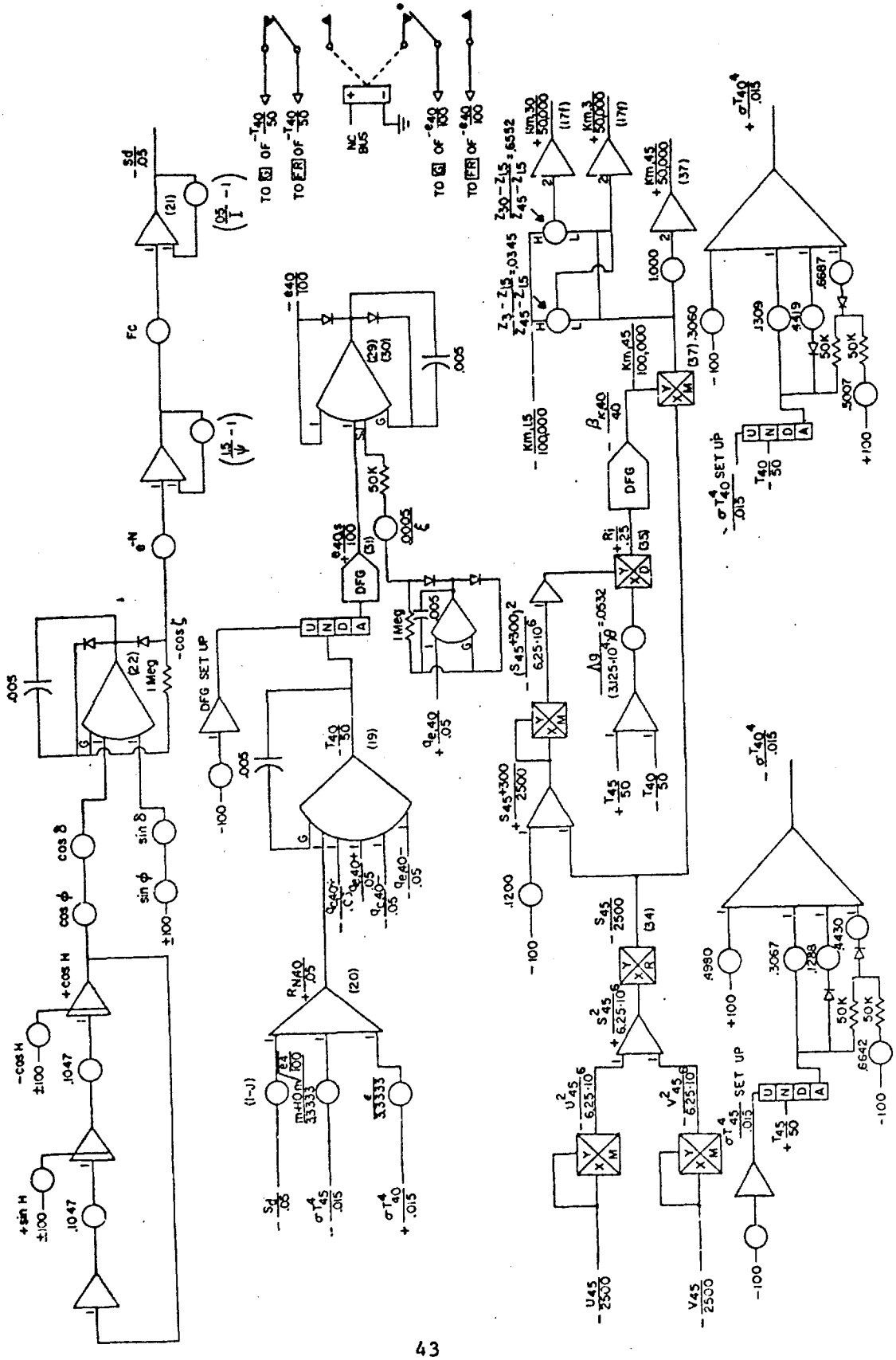

FOREST CANOPY ENERGY BALANCE

appears on a series potentiometer to obtain cos ϕ cos δ cos [15(t - 12)], the second term in equation (s22). The first term of this equation is calculated with two series potentiometers. The first potentiometer is set equal to sin ϕ, and the second potentiometer is set to the value of sin δ to obtain the product sin ϕ sin δ at the arm of the second potentiometer. These two terms are summed in an amplifier which has a gain of unity for positive inputs and a gain of zero for negative inputs; therefore, the output of this amplifier is -cos ζ for the hours of daylight and zero at night. The output of this amplifier is applied to a potentiometer set to -N so as to calculate e^{-N} cos ζ. This product is further multiplied by the solar distance factor which is calculated through the use of a potentiometer as an additional feedback on a summing amplifier. Multiplication by F_c and I are accomplished by a coefficient potentiometer set to F_c and an amplifier with its feedback modified by a potentiometer set to [(.05/I)-1].

Inspection of the equations for the free air canopy reveals that each equation is implicit in the temperature at the top of the canopy $T_d/50$; therefore, a value of $T_d/50$ must be found that satisfies the energy balance equation at the top of the canopy.* Since the effect of $T_d/50$ is algebraically the same in each equation, the solution diagram is equivalent, analog wise, to having a negative feedback around a high-gain amplifier for which the inputs are the energy balance terms. This condition may be expressed as

*The subscript d is equivalent to the height of 40 m on the wiring schematics.

$-T_d/50 = K(R_N/.05 - q_{c,d+}/.05 - q_{e,d+}/.05 - q_{c,d-}/.05 - q_{e,d-}/.05)$

where K is the open loop gain of the amplifier.

If there is a state of balance for this feedback network, there is a solution for this set of equations in terms of T_d. The high gain of the amplifier will force the sum of the inputs to be zero and the amplifier output will be $-T_d/50$.

There are three feedback loops for the $-T_d/50$ amplifier.

1. The output of the $-T_d/50$ amplifier is applied to the neutral position of the function switch and further to the input of the patchboard function generator which calculates $+\sigma T_d^4/.015$. The output of this function generator is applied to a potentiometer having $\varepsilon/3.333$ as its setting. The resulting product, $+\varepsilon\sigma T_d^4/.05$, is added to $-\sigma T_{45}^4(m + 10n\sqrt{e_d/100})/.05$ and $-(1 - J)S_d/.05$ to obtain the net radiation at height d. $R_{N,d}/.05$ is further fed back into the $-T_d/50$ amplifier to complete the loop.

2. The output of the $-T_d/50$ amplifier is applied to the neutral position of a function switch and thence into the input of a variable diode function generator which has as output $+e_{d,s}/100$. The saturation vapor pressure is fed to another high-gain amplifier which has an additional input of $-q_{e,d+}/100\varepsilon$. This additional input provides the polarity constraint for saturated or unsaturated conditions. The output of the high-gain amplifier is $-e_d/100$ which is further applied to 10-gain inputs of two high gain amplifiers on page 55, which have as outputs $+(q_{e,d+}/.05)/(K_{m,45}/50,000)$ and $-(q_{e,d-}/.05)/(K_{m,45}/50,000)$. These values are multiplied by $K_{m,45}/50,000$ by use of servomultipliers.

The resulting values of $+q_{e,d+}/.05$ and $-q_{e,d-}/.05$ are inverted with a unity-gain amplifier, and both values of the vapor flux are fed back into unity-gain inputs of the $-T_d/50$ amplifier.

3. The third negative feedback loop results from the calculation of the convective heat flux. This feedback loop is shown on pages 43 and 51. The output of the $-T_d/50$ amplifier is applied to 10-gain inputs on two high-gain amplifiers appearing on page 51. The output of each of these amplifiers is fed to the high side of a servomultiplier, the outputs of which are $+q_{c,d+}/.05$ and $-q_{c,d-}/.05$. These two values, subsequently, are fed back to the inputs of the $-T_d/50$ amplifier to complete the feedback loop.

The .005 mfd capacitors used as feedback elements around the high-gain amplifiers which compute $-T_d/50$ and $-e_d/100$ are of no computational significance. These feedback elements are used extensively throughout the wiring diagrams for noise suppression. The low speed relay shown on the right of the diagram on page 41 is used simply to provide feedback on the $-T_d/50$ and $-e_d/100$ high gain amplifiers while the computer is in the balance mode.

The circuit diagram for calculating the momentum exchange coefficients at 3, 30, and 45 m height is shown at the bottom of page 43. This circuit calculates equations s34 through s37. In the lower left-hand corner of page 43 $-u_{45}/2500$ and $-v_{45}/2500$ are independently connected to the x and y inputs of two electronic multipliers. The outputs of these multipliers $-u_{45}^2/6.25 \times 10^6$ and $-v_{45}^2/6.25 \times 10^6$ are further added in a summing amplifier to get $+S_{45}^2/6.25 \times 10^6$, the square of the magnitude of the vector wind. The square root c

$+S_{45}^2/_2 6.25 \times 10^6$ is obtained by an electronic multiplier used in square root mode. The output $-S_{45}/2500$ of this electronic multiplier is applied to a unity gain input on a summing amplifier and to the x input of another electronic multiplier. The quantity $+(S_{45} + a)/2500$ is calculated by adding $-S_{45}/2500$ and $-a/2500$ in the summing amplifier. The quantity a is chosen to be 3 m/sec. This sum is further applied to both the x and y inputs of an electronic multiplier to calculate $-(S_{45} + a)^2/6.25 \times 10^6$. This value then is inverted in sign and applied to the y input of an electronic multiplier.

The temperatures $+T_{45}/50$ and $-T_d/50$ are added in a summing amplifier and multiplied by $g/3.125 \times 10^4 \theta$ set on a potentiometer. The resulting product is applied to the x input of an electronic multiplier in divide mode which has as its y input $-(S_{45} + a)^2/6.25 \times 10^6$. The quotient obtained is the modified Richardson number. The modified Richardson number is then applied to the input of the function generator containing $-\beta_{\kappa,4}/40$ as its output. This quantity is applied further to the y input of an electronic multiplier having as its x input $-S_{45}/2500$. The multiplication of these two terms yields the momentum exchange coefficient at 45 m height.

The calculation of the exchange coefficient for momentum at 1.5-m height is completely analogous to that at 45 m. Linear interpolation is used between 1.5 m and 45 m to calculate the values for $K_{m,3}$ and $K_{m,30}$.

The solutions of the equations for the forest surface section are similar to those for the air canopy section except, in that case,

the equations are implicit in the surface temperature of the ground, $-T_o/50$. This program appears on page 49.

For the surface section, an integral exchange coefficient is employed. The diagram for the calculation of this parameter is shown on the lower right-hand side of page 49. The input of $+R_i/.25$ is fed to the function generator containing $\beta_\delta/.006$ as an output. This output is further applied to the x input of an electronic multiplier having as its y input $-S_{1.5}/1000$; the resulting product is $-D_{1.5}/10$.

A simplified soil structure is employed in the forest surface section. Its analog solution diagram is found on the left edge and near the center on page 49. The soil surface temperature $+T'_o/50$ is obtained from an integrator having inputs of the soil heat flux, $-q_{s,o}/.01$, multiplied by $2\sqrt{\pi/P\mu\lambda}$ set on a potentiometer, $+T'_o/50$ applied in a negative feedback loop to a potentiometer for which the setting is $2\pi/P$, and the mean representative temperature for the soil also multiplied by $2\pi/P$ set on a potentiometer.

The temperatures are calculated from equations s3 and s3f and are shown in diagrammatic form on page 50. The solutions are completely analogous to those for obtaining the winds discussed earlier. The radiation term R is calculated in the lower left hand corner of page 51, and the value $\pm R/.03472$ is applied to potentiometers feeding the individual integrators. This arrangement permits the variation of R with height and forest structure. Temperature advection terms are handled in exactly the same manner as are the wind advection terms.

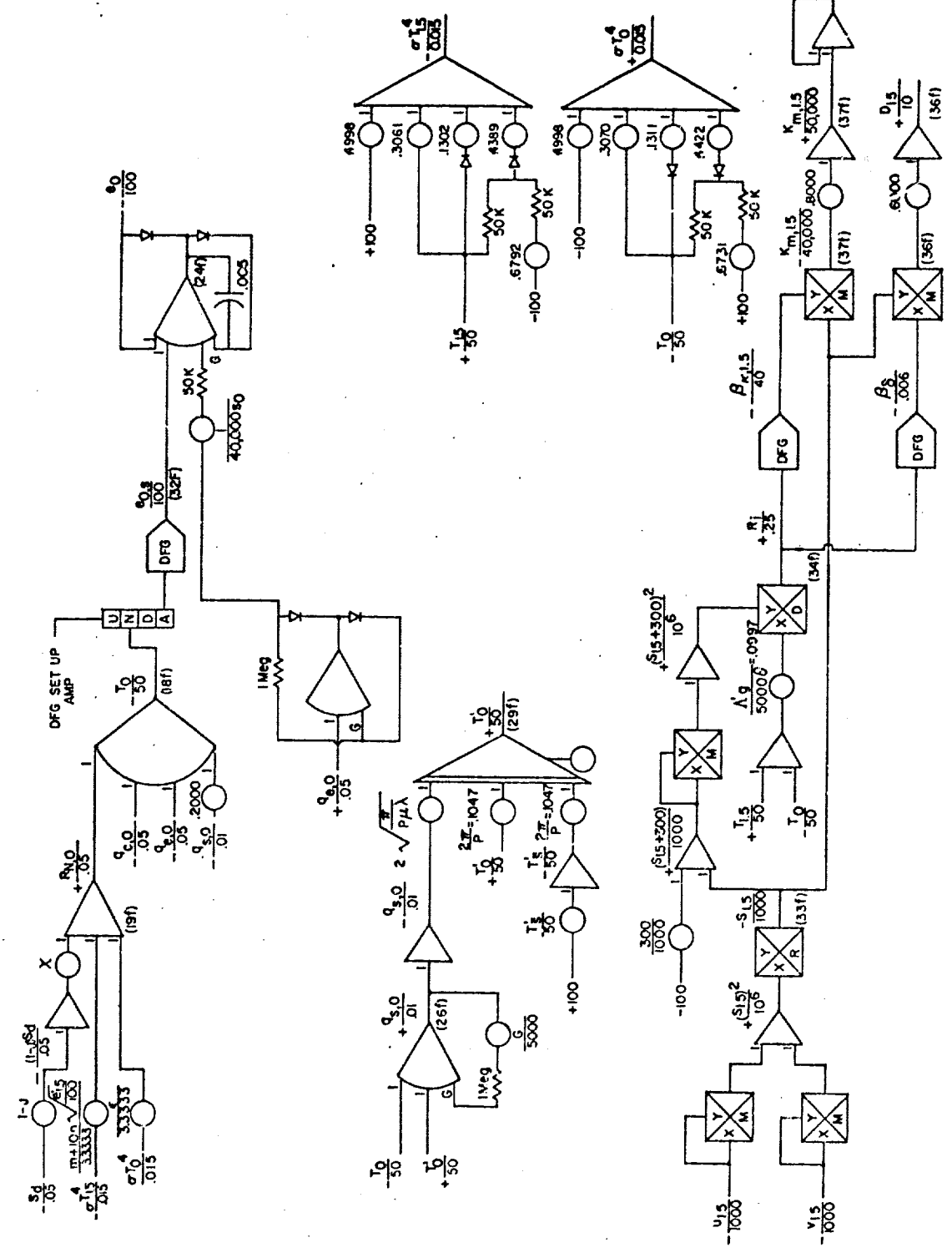
DFG SET UP AMP
DFG
SURFACE ENERGY BALANCE

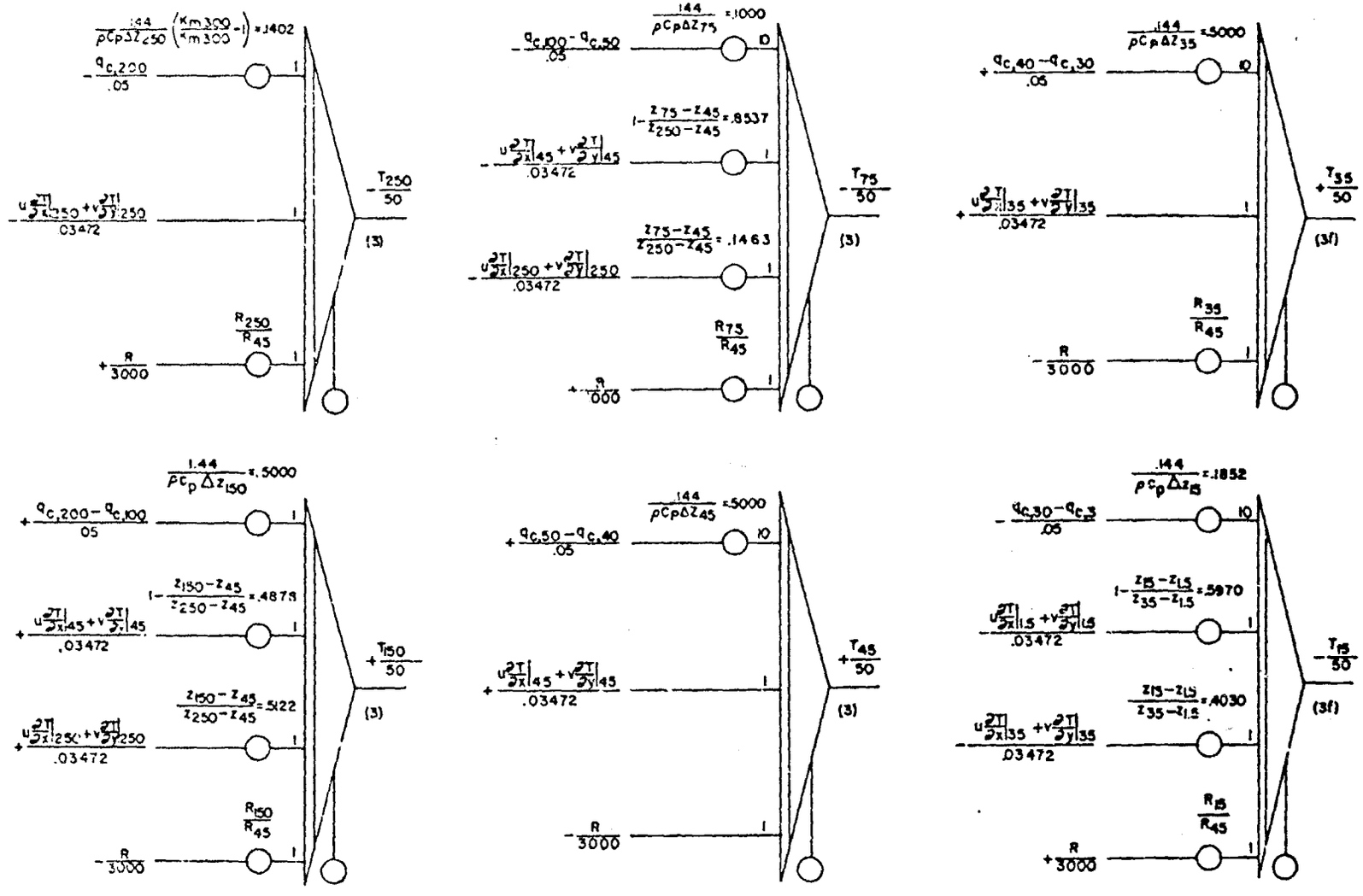

AIR TEMPERATURES

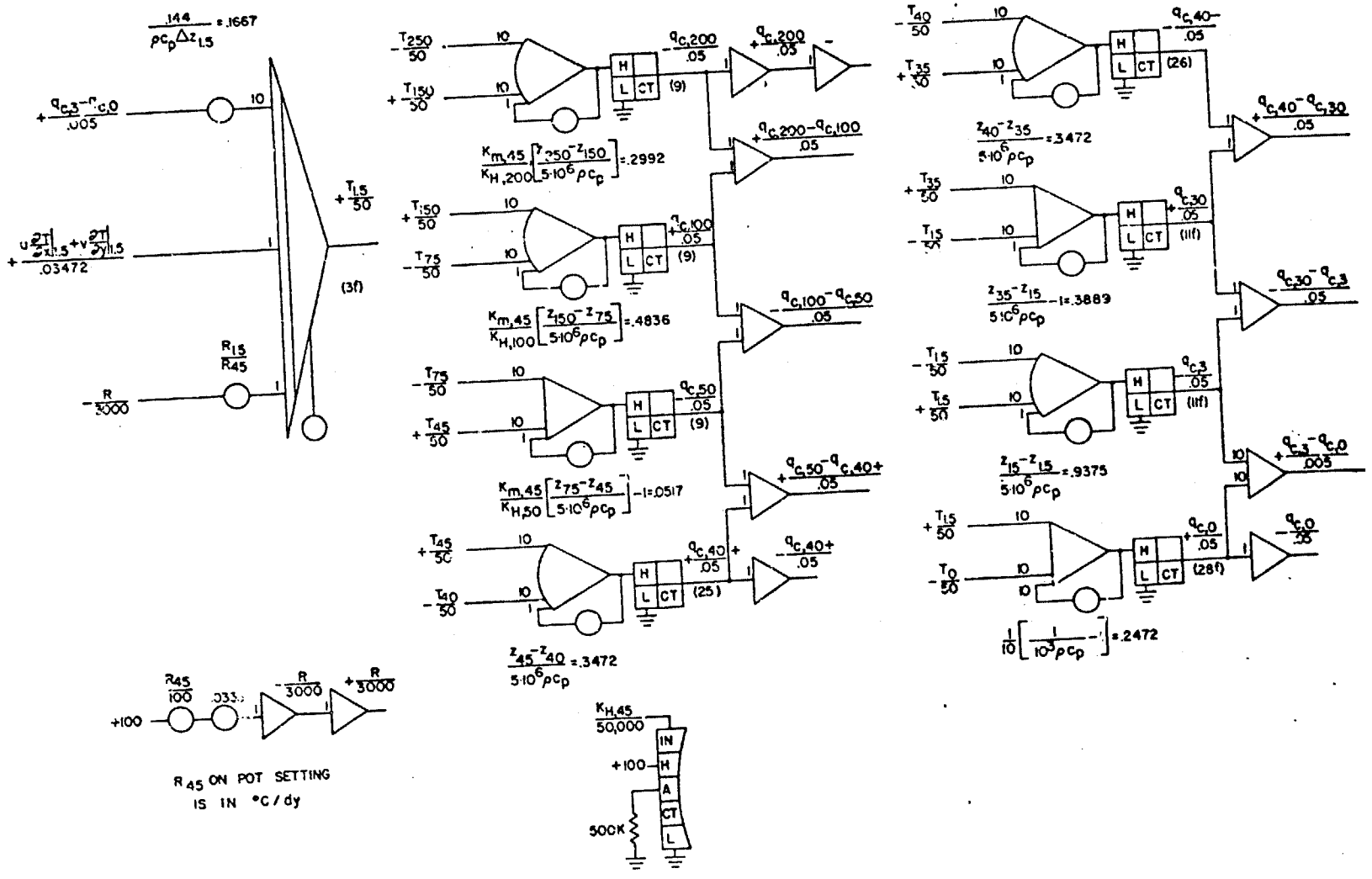
.144 / ρc_pΔz_1.5 = .1667
(3f)
R_45 ON POT SETTING IS IN °C / dy
FLUXES OF CONVECTIVE HEAT
(9)
(25)
(26)
(11f)
(28f)
500K

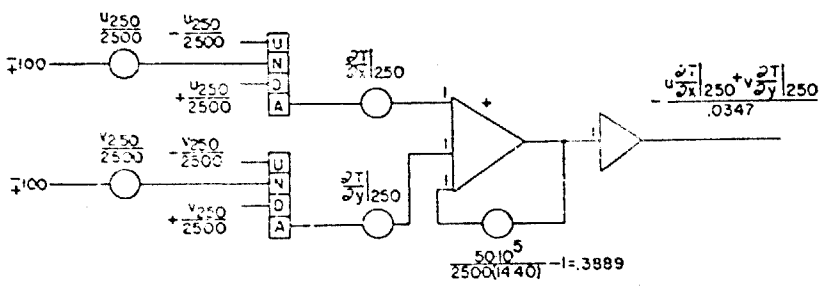

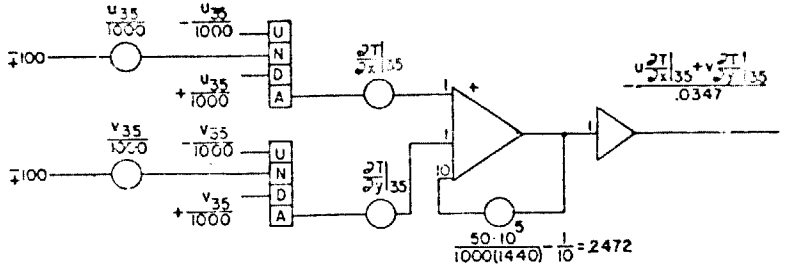

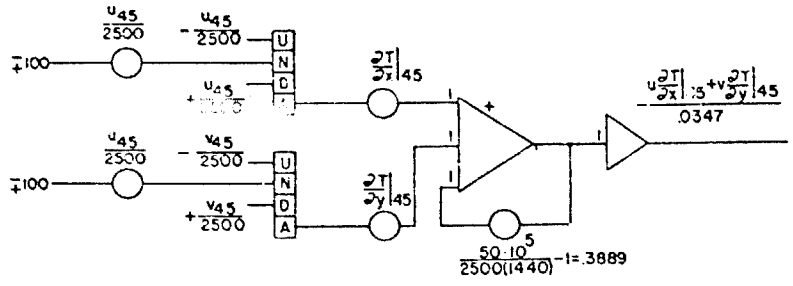

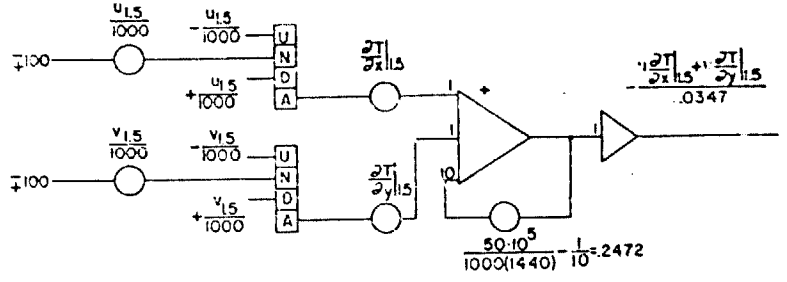

$\partial T/\partial x$ AND $\partial T/\partial y$ ARE IN °C/km

ADVECTION OF TEMPERATURE

The diagrams for calculating vapor pressures are shown on page 54 and are seen to be completely analogous to the calculations of temperature and wind components. The only term that is significantly different from the others is the moisture term which is calculated on the lower left-hand corner of page 55. This term applies only within the forest where trees and brush act as moisture sources.

This set of solution diagrams represents only an initial step toward the development of an analog system for simulating the behavior of the atmosphere within and above a tropical forest. Equation refinement with resulting modifications in the solution diagrams will be required since little factual information exists concerning many of the parameters employed to describe the forest and functional definitions are essentially nonexistant.

The moisture source term, M, presently being employed as a constant requires functional definition as does the radiation term R. In addition, the magnitude of the drag coefficient C_D is not known for air flow below the forest canopy; therefore, for lack of better information, a value is being employed that is representative of flow over rough surfaces.

The exchange coefficients for momentum, heat, and vapor, now defined by the Deacon wind profile, may need redefinition for forest application. In this regard, the roughness of the forest canopy will require reformulation in order to be compatible with Deacon's wind profile.

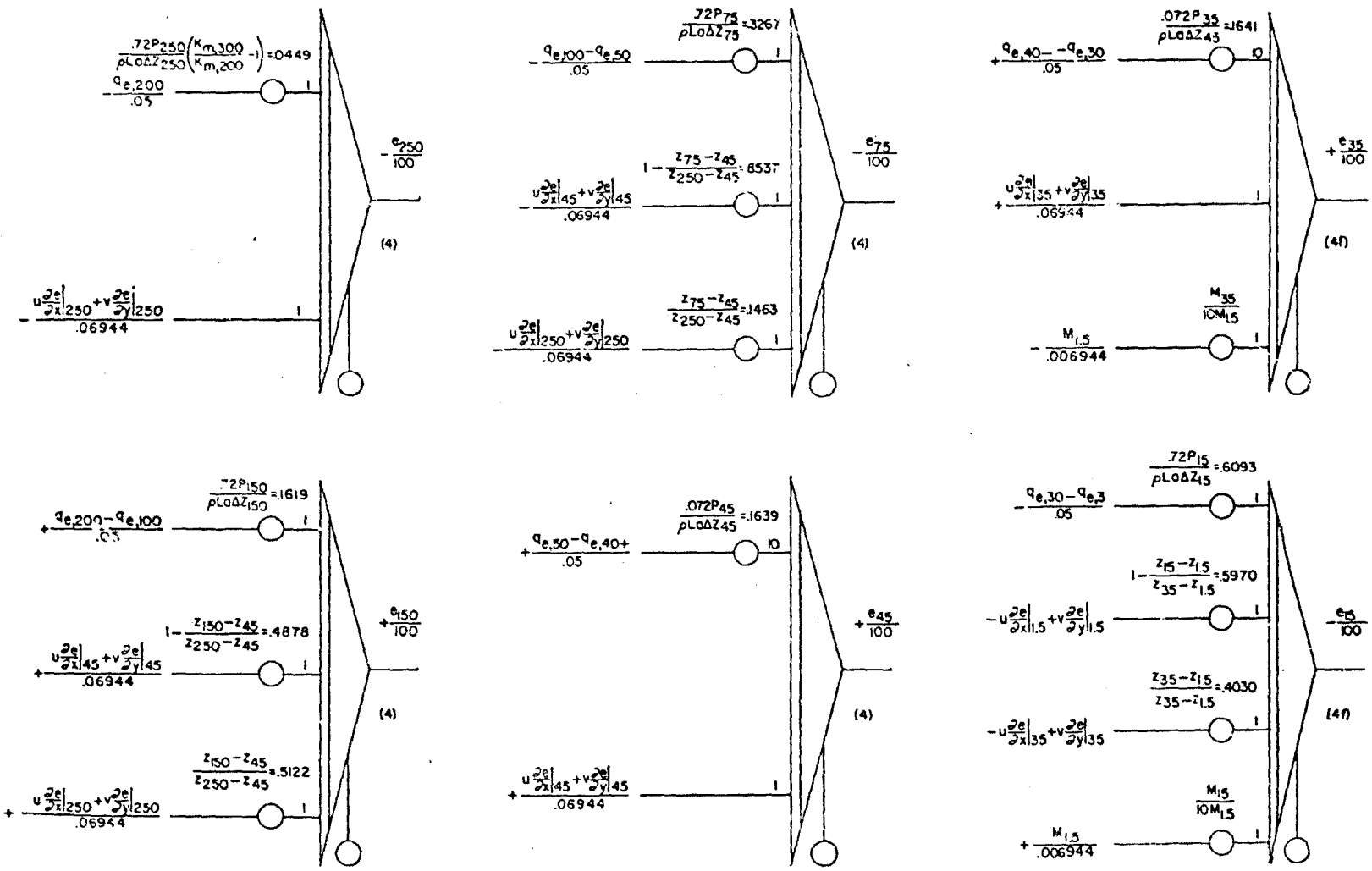

VAPOR PRESSURES

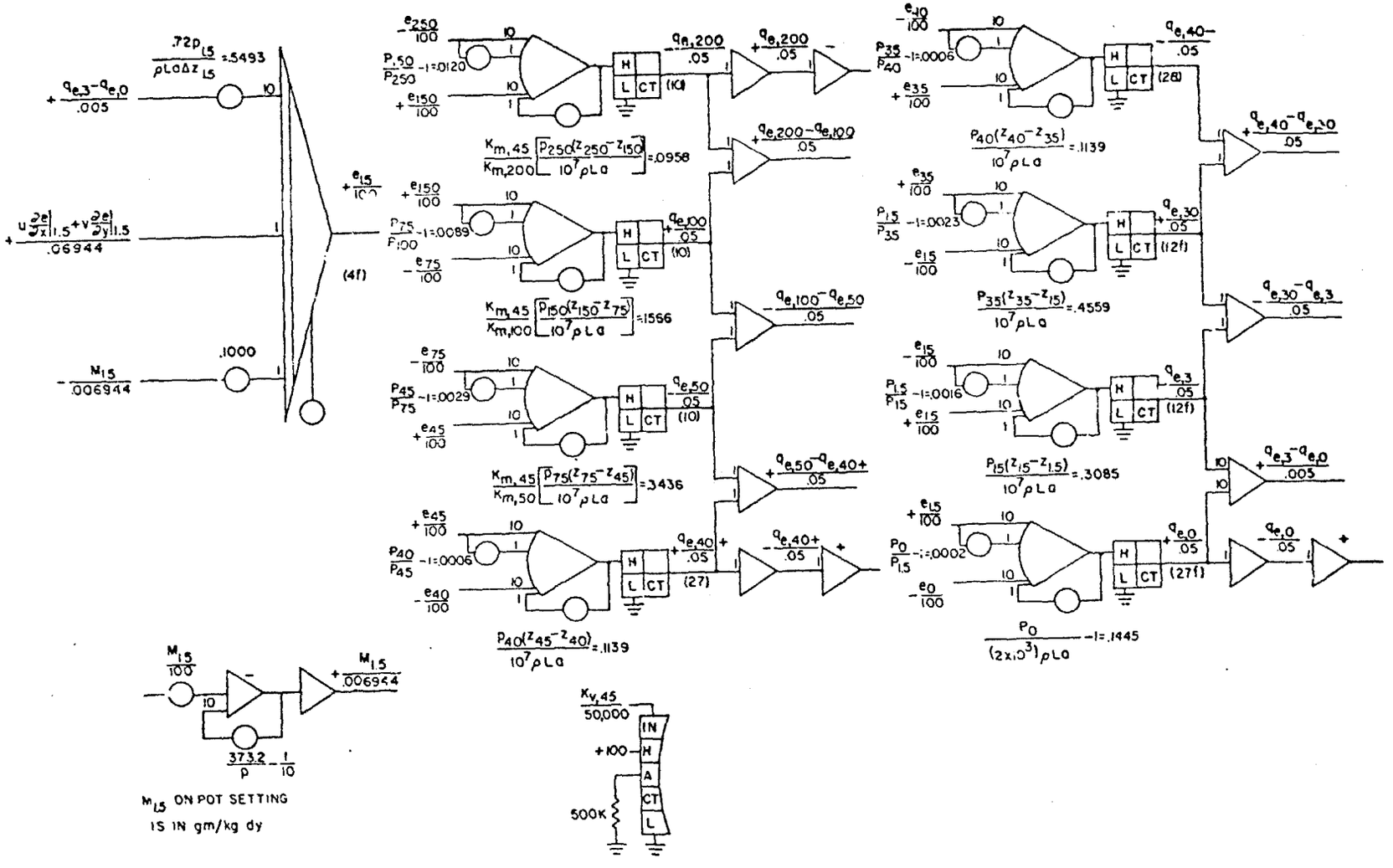

FLUXES OF EVAPORATIVE HEAT

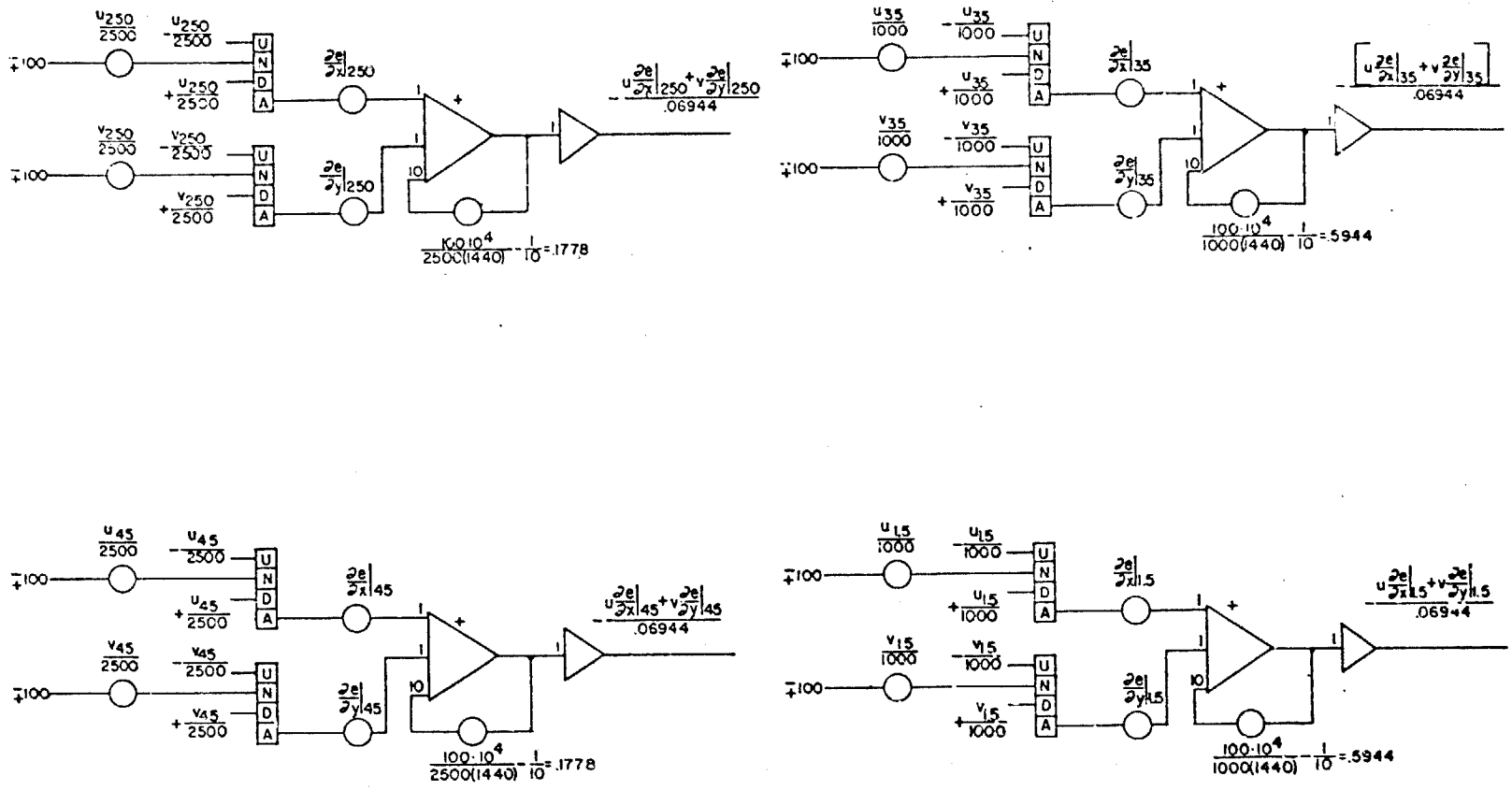

$\partial e/\partial x$ AND $\partial e/\partial y$ ARE IN mb/km.

ADVECTION OF VAPOR PRESSURE

V. Engineering Activities

During the past six months, the major engineering accomplishments have consisted of the completion of the new test jig for checking the individual computing components for the general purpose analog computer (GPAC), the installation of a completely new grounding system for the GPAC, and the installation of a new enclosed relay rack which will contain the five diode function generators presently in use and three additional ones. Other engineering tasks, not as large but just as important, were completed during this reporting period. Two trunk lines were run from Console 4 of the GPAC into the electronics shop for use with the new test jig. All of the integrators on the GPAC were adjusted again for proper rates of integration. All of the servomultipliers and servoresolvers were checked for alignment and for worn bearings, gears, and potentiometers. Three of these servos required rebuilding. In addition, the necessary relays and switches were added to the GPAC remote control box to permit control of Console 5 simultaneously with Consoles 1 through 4.

Work was begun on updating and drafting of wiring diagrams for project equipment in use and on setting up a suitable procedure for indexing all wiring schematics for easy filing and ready reference.

New equipment received included a six channel Brush recorder, a BRPE Teletype Corporation High Speed Tape Punch, a Fluke model 335 voltage standard, and a Fluke model 8300 digital voltmeter.

LIST OF SYMBOLS

A	characteristic tree coverage	(cm^{-1})
a	ratio of molecular weight of water to molecular weight of dry air	(gm/gm)
C_D	local drag coefficient	(non-dimensional)
C'_D	forest drag coefficient ($C'_D = AC_D$)	(cm^{-1})
C_p	specific heat of air at constant pressure	(cal/gm deg)
$K_{z'}$	integral exchange coefficient for momentum between surface and height z'	(cm)
d	height of the effective top of the canopy	(cm)
e	mean vapor pressure for a subscripted layer	(mb)
e'	representative vapor pressure	(mb)
$e_{d,s}$	saturation vapor pressure at the temperature of the canopy top	(mb)
$e_{o,s}$	surface saturation vapor pressure	(mb)
F_c	cloud factor for insolation	(non-dimensional)
FCG	forecast height contour gradient	(m/100 km)
(FCG)	angle made by the forecast height contour gradient with the y-axis	(deg)
F_x, F_y	components of drag force per unit volume of air due to trees and foliage	$(dynes/cm^3)$
f	Coriolis parameter	(rad/sec)
G	thermal conductivity of surface litter	$(cm^2 sec\ deg/cal)$
g	acceleration due to gravity	(cm/sec^2)
h	hour angle (zero for local apparent noon)	(deg)
h	height of a constant pressure surface	(cm)
I	mean solar constant	$(cal/cm^2 sec)$
ICG	initial contour gradient	(m/100 km)

(ICG)	angle made by the initial contour gradient vector with the y-axis	(deg)
i,j,k	indices	
J	albedo	(non-dimensional)
K_h	exchange coefficient for heat	(cm^2/sec)
K_m	exchange coefficient for momentum	(cm^2/sec)
K_v	exchange coefficient for water vapor	(cm^2/sec)
k	.40 (Von Karman's constant)	(non-dimensional)
L	latent heat of vaporization of water	(cal/gm)
L_N	net longwave radiation	(cal/cm^2sec)
M	moisture source term for forest	(mb/sec)
m	empirical radiation factor	(non-dimensional)
N	turbidity	(non-dimensional)
n	empirical radiation factor	($mb^{-1/2}$)
P	86,400 (diurnal period)	(sec)
p	atmospheric pressure	(mb)
Q	energy addition per unit mass from non-adiabatic processes	(cal/gm)
q_c	convective heat flux, positive upward	(cal/cm^2sec)
$q_{c,d+}$	convective heat flux in air layer just above canopy, positive upward	(cal/cm^2sec)
$q_{c,d-}$	convective heat flux in canopy just below the level d, positive downward	(cal/cm^2sec)
q_e	evaporative heat flux, positive upward	(cal/cm^2sec)
$q_{e,d+}$	evaporative heat flux in air layer just above canopy, positive upward	(cal/cm^2sec)
$q_{e,d-}$	evaporative heat flux in canopy just below the level d, positive downward	(cal/cm^2sec)

q_s	soil heat flux, positive downward	(cal/cm^{2}sec)
R	radiational cooling or warming	(deg/sec)
R_d	gas constant for dry air	(cm^2/sec^{2}deg)
R_N	net radiation	(cal/cm^{2}sec)
r	mean specific humidity for a subscripted layer	(gm/gm)
S	mean wind speed for a subscripted layer	(cm/sec)
S_N	net shortwave radiation	(cal/cm^{2}sec)
s_o	surface moistness	(cal/cm^{2}sec mb)
T	mean temperature of air for a subscripted layer	(deg C)
T'	mean soil temperature for a subscripted layer	(deg C)
$T'_{\bar{S}}$	representative soil temperature	(deg C)
T_d	dewpoint temperature	(deg C)
t	time	(sec)
u	mean east-west component of wind for a subscripted layer	(cm/sec)
v	mean north-south component of wind for a subscripted layer	(cm/sec)
u_g, v_g	geostrophic wind components	(cm/sec)
x	east-west coordinate, positive eastward	(cm)
y	north-south coordinate, positive northward	(cm)
z_i	105,000, top of boundary layer	(cm)
z	vertical coordinate, positive upward	(cm)
z_o	surface roughness length	(cm)
zero	as a subscript indicates value at z = 0 excepting s_o and z_o	
λ'	gradient of wind along streamline	(sec^{-1})

ξ	stability parameter of the beacon profile	(non-dimensional)
τ'	ratio of wind speed to radius of curvature of streamline	(sec^{-1})
δ	solar declination	(deg)
Δh	vertical interval between mean heights of adjacent simulator layers	(cm)
Δt	increment of time	(sec)
Δz_j	mean vertical thickness of the j^{th} layer	(cm)
ε	emissivity	(non-dimensional
ζ	solar zenith angle	(deg)
θ	mean potential temperature for a subscripted layer	(deg K)
Λ	1/2 depth of air-canopy layer	(cm)
Λ'	depth of forest surface layer	(cm)
λ	volumetric heat capacity of soil	($cal/cm^3 deg$)
μ	thermal conductivity of soil	(cal/cm sec deg)
ξ	moisture parameter for the canopy	($cal/cm^2 sec$ mb)
π	3.14. . . .	(non-dimensional)
ρ	1.2×10^{-3}, air density	(gm/cm^3)
σ	1.354×10^{-12}, Stefan Boltzmann constant	($cal/cm^2 sec\ deg^4$)
τ_x	component of τ in x direction	($dynes/cm^2$)
τ_y	component of τ in y direction	($dynes/cm^2$)
ϕ	latitude	(deg)
χ	forest transmissivity	(non-dimensional)
ψ	solar distance factor	(non-dimensional)
ω	7.3×10^{-5} (angular velocity of earth's rotation)	(rad/sec)

Security Classification

DOCUMENT CONTROL DATA - R & D

Security classification of title, body of abstract and indexing annotation must be entered when the overall report is classified)

1. ORIGINATING ACTIVITY (Corporate author) Texas A & M Research Foundation College Station, Texas	2a. REPORT SECURITY CLASSIFICATION 2b. GROUP

3. REPORT TITLE

Evaluation of Atmospheric Transport and Diffusion

4. DESCRIPTIVE NOTES (Type of report and inclusive dates)

Fourth Semi-Annual Report for 15 December 1969 to 15 June 1970

5. AUTHOR(S) (First name, middle initial, last name)

Tom E. Sanford

6. REPORT DATE	7a. TOTAL NO. OF PAGES	7b. NO. OF REFS
September 1970	73	None

8a. CONTRACT OR GRANT NO DAAB07-68-C-0381 b. PROJECT NO. 586 c. d.	9a. ORIGINATOR'S REPORT NUMBER(S) 70-9-T 9b. OTHER REPORT NO(S) (Any other numbers that may be assigned this report) ECOM-0381-4

10. DISTRIBUTION STATEMENT

This document is subject to special export controls and each transmittal to foreign governments of foreign nationals may be made only with prior approval of CG, U.S. Army Electronics Command, Fort Monmouth, New Jersey ATTN: AMSEL-BL-FM-T

11. SUPPLEMENTARY NOTES	12. SPONSORING MILITARY ACTIVITY
	U. S. Army Electronics Command Fort Monmouth, New Jersey 07703 AMSEL-BL-FM-T

13. ABSTRACT

This report contains a summary of the activities carried out under Signal Corps Contract No. DAAB07-68-C-0381 (Texas A & M Research Foundation Project No. 586) during the contract period 15 December 1969 to 15 June 1970.

Activities during this period have been devoted primarily to the programming of the equations for the forested boundary layer and the wiring and checking of the computer patchboards for solution of these equations on the general analog computer at Texas A&M University. The complete set of these equations scaled in analog format is included in this report as are wiring diagrams for solution of the scaled equations.

DD FORM 1473 (PAGE 1)

S/N 0101-807-6811

Security Classification

A-31408

14. KEY WORDS	LINK A		LINK B		LINK C	
	ROLE	WT	ROLE	WT	ROLE	WT
1. Meteorology						
2. Atmospheric Transport and Diffusion						
3. Department of the Army Contract No. DAAB07-68-C-0381						